Received: 16 June 2020 | Revised: 10 August 2020 | Accepted: 11 August 2020

DOI: 10.1002/dta.2913

RESEARCH ARTICLE

WILEY

Synthetic cannabinoid receptor agonists: Analytical profiles and development of QMPSB, QMMSB, QMPCB, 2F-QMPSB, QMiPSB, and SGT-233

Simon D. Brandt[1] | Pierce V. Kavanagh[2] | Folker Westphal[3] | Wolfgang Dreiseitel[4] | Geraldine Dowling[2,5] | Matthew J. Bowden[6] | James P.B. Williamson[7]

[1]School of Pharmacy and Biomolecular Sciences, Liverpool John Moores University, Liverpool, UK

[2]Department of Pharmacology and Therapeutics, School of Medicine, Trinity Centre for Health Sciences, St. James Hospital, Dublin, Ireland

[3]Section Narcotics/Toxicology, State Bureau of Criminal Investigation Schleswig-Holstein, Kiel, Germany

[4]Hessian State Bureau of Criminal Investigation, Wiesbaden, Germany

[5]Department of Life Sciences, School of Science, Sligo Institute of Technology, Ash Lane, Sligo, Ireland

[6]Stargate International, Auckland, New Zealand

[7]Synex Synthetics BV, Maastricht, The Netherlands

Correspondence
Simon D. Brandt, School of Pharmacy and Biomolecular Sciences, Liverpool John Moores University, Byrom Street, Liverpool L3 3AF, UK.
Email: s.brandt@ljmu.ac.uk

Abstract

A diverse assortment of molecules designed to explore the cannabinoid receptor system and considered new psychoactive substances (NPS) have become known as synthetic cannabinoid receptor agonists (SCRAs). One group of SCRAs that has received little attention involves those exhibiting sulfamoyl benzoate, sulfamoyl benzamide, and *N*-benzoylpiperidine based structures. In this study, quinolin-8-yl 4-methyl-3-(piperidine-1-sulfonyl)benzoate (QMPSB), quinolin-8-yl 4-methyl-3-(morpholine-4-sulfonyl) benzoate (QMMSB), quinolin-8-yl 4-methyl-3-(piperidine-1-carbonyl)benzoate (QMPCB, SGT-11), quinolin-8-yl 3-(4,4-difluoropiperidine-1-sulfonyl)-4-methylbenzoate (2F-QMPSB, QMDFPSB, SGT-13), quinolin-8-yl 4-methyl-3-[(propan-2-yl)sulfamoyl] benzoate (QMiPSB, SGT-46), and 3-(4,4-difluoropiperidine-1-sulfonyl)-4-methyl-*N*-(2-phenylpropan-2-yl)benzamide (SGT-233) were extensively characterized (including data on impurities). The analytical profiles may be useful to researchers and scientists who deal with the emergence of NPS during forensic and clinical investigations. The detection of QMPSB was first published in 2016 but it is worth noting that Stargate International, a company originally formed to develop harm reduction solutions, were involved in the investigation and development of these six compounds for potential release between 2011 and early 2014. Whilst information on the prevalence of use of these particular compounds at the present time is limited, one of the key outcomes of the research performed by Stargate International reviewed here was to set the stage for the quinolin-8-yl ester head group that ultimately led to hybridization with an *N*-alkyl-1*H*-indole core to give SGT-21 and SGT-32, which became later known as PB-22 (QMPSB/JWH-018 hybrid) and BB-22, respectively, thus, opening the door to a range of SCRAs carrying the quinolin-8-yl head group from about 2012 onwards.

KEYWORDS

analysis, history, NPS, research chemicals, synthetic cannabinoids

1 | INTRODUCTION

Since the initial discovery of pravadoline and WIN 55,212-2 in the late 1980s and their subsequent identification as cannabinoid receptor agonists in the mid-1990s,[1,2] several thousand synthetic cannabinoid receptor agonists (SCRAs) of the same basic "tail-core-linker-head" chemotype[3,4] have been reported. Reviews in this field (eg, Huffman and Padgett,[5] Manera et al.,[6] Wiley et al.,[7] Banister and Connor,[8,9] and Alam and Keating[10]) indicate that many of these substances originated within university settings for pharmacological research into cannabinoid receptors and their downstream signaling systems.

The majority of compounds in this class have been claimed in pharmaceutical patents with a variety of suggested applications. The preponderance of SCRAs originating from pharmaceutical patents has not escaped the attention of "designer drug" vendors looking to market these compounds for recreational use. For example, a pair of patents from 2009 issued to Pfizer Inc. list hundreds of potent CB_1R agonists from the indazole-3-carboxamide group along with their synthetic routes and associated in vitro activity data.[11,12] Some of these have subsequently been identified as new psychoactive substances (NPS) along with various related derivatives obtained by minor modifications, such as the replacement of the indazole core and fluorination of the tail group. By the end of the 2010s, various highly potent and inexpensively manufactured SCRAs from this group were prominent on the SCRA market around the world.[13,14]

An important aspect of SCRA research involves the evaluation of substances that either have limited ability to penetrate the blood–brain barrier or are relatively CB_2R-selective in an effort to prevent cannabis-like psychoactive effects mediated by the activation of CB_1R located in the brain. On the other hand, numerous SCRAs suggested to be peripherally selective[15] or highly CB_2R selective[16,17] have nevertheless appeared on the global market and reportedly induce psychoactive effects in people who use these substances.

The majority of SCRAs identified on the market so far are substances incorporating a bi- or tricyclic core (eg, indoles, indazoles, azaindoles, carbazoles, benzimidazoles, γ-carbolines).[8,9] Despite the plethora of compounds in the scientific literature, few monocyclic core SCRAs have appeared as street drugs to date. However, examples that include the identification of substances having pyrrole (eg, JWH-030 and JWH-307[18]), thiazole (A-836,339),[19] or pyrazole cores (AB-CHFUPYCA/5,3-AB-CHFUPYCA,[20,21] 5F-AB-FUPPYCA,[22] AMPPPCA, and 5F-AMPPPCA[23] (Figure 1A) exist. The extent to which such novel pyrazole SCRAs exhibit any CB_1R/CB_2R agonist activity remains to be explored given that some cannabinoid ligands with a pyrazole core are also known as cannabinoid receptor inverse agonists/antagonists such as rimonabant and AM-251.[24] Several agonist derivatives, such as O-1269[25] and a number of dihydropyrazoles,[26,27] or examples where the pyrazole ring is fused with bicyclo[2.2.1]heptane[28] (Figure 1B) are also known.

Another group of mixed CB_1R/CB_2R agonists with a monocyclic core is based on a template that includes a sulfamoyl benzoate or sulfamoyl benzamide structure. One such compound is quinolin-8-yl 4-methyl-3-(piperidine-1-sulfonyl)benzoate (QMPSB, **1**) (Figure 1C), a sulfamoyl benzoate that was identified as a constituent in seized herbal material and reported in 2016.[29] The identification of SCRAs remains to be a relevant undertaking when facing the emergence of NPS across the fields related to substance use. In the present investigation, detailed analytical characterizations are presented to complement the existing information on QMPSB (**1**)[29] and to provide new data on the closely related SCRAs: quinolin-8-yl 4-methyl-3-(morpholine-4-sulfonyl)benzoate (QMMSB) (**5**), quinolin-8-yl 4-methyl-3-(piperidine-1-carbonyl)benzoate (QMPCB, SGT-11) (**14**), quinolin-8-yl 3-(4,4-difluoropiperidine-1-sulfonyl)-4-methylbenzoate (2F-QMPSB, QMDFPSB, SGT-13) (**17**), quinolin-8-yl 4-methyl-3-[(propan-2-yl)sulfamoyl]benzoate (QMiPSB, SGT-46) (**19**), and 3-(4,4-difluoropiperidine-1-sulfonyl)-4-methyl-*N*-(2-phenylpropan-2-yl)benzamide (SGT-233) (**22**) (Figure 1C), and data on impurities. This report also shows that these six substances were first made available between late 2011 and early 2014. These were investigated by Stargate International, a company originally formed to develop harm reduction solutions and drugs for therapeutic applications, which set the stage for the quinolin-8-yl ester head group that ultimately led to hybridization with an *N*-alkyl-1*H*-indole core to yield SGT-21 and SGT-32, which became known as PB-22 (**28**) and BB-22 (**29**), respectively, thus opening the door to a range of SCRAs carrying the quinolin-8-yl head group from about 2012 onwards.

2 | EXPERIMENTAL

2.1 | Materials

All chemicals used for the analysis were obtained from Merck (Arklow, Ireland) or Merck (Dorset, UK). The six analytes undergoing analytical characterization were obtained from the library of Stargate International (Auckland, New Zealand).

2.2 | Instrumentation

2.2.1 | Gas chromatography–mass spectrometry (GC-MS)

For electron ionization mass spectrometry (EI-MS) and electron ionization tandem mass spectrometry (EI-MS/MS), a Finnigan TSQ 8000 Evo triple stage quadrupole mass spectrometer coupled to a gas chromatograph (Trace GC 1310, Thermo Electron, Dreieich, Germany), and for chemical ionization mass spectrometry (CI-MS and chemical ionization tandem mass spectrometry (CI-MS/MS), a Finnigan TSQ 7000 triple stage quadrupole mass spectrometer coupled to a gas chromatograph (Trace GC Ultra, Thermo Electron, Dreieich, Germany) were used. A Triplus RSH (Thermo Scientific for TSQ 8000 Evo) and a CTC CombiPAL (CTC Analytics, Zwingen, Switzerland for TSQ 7000) autosampler were employed for sample introduction. Mass spectra were recorded at an electron ionization

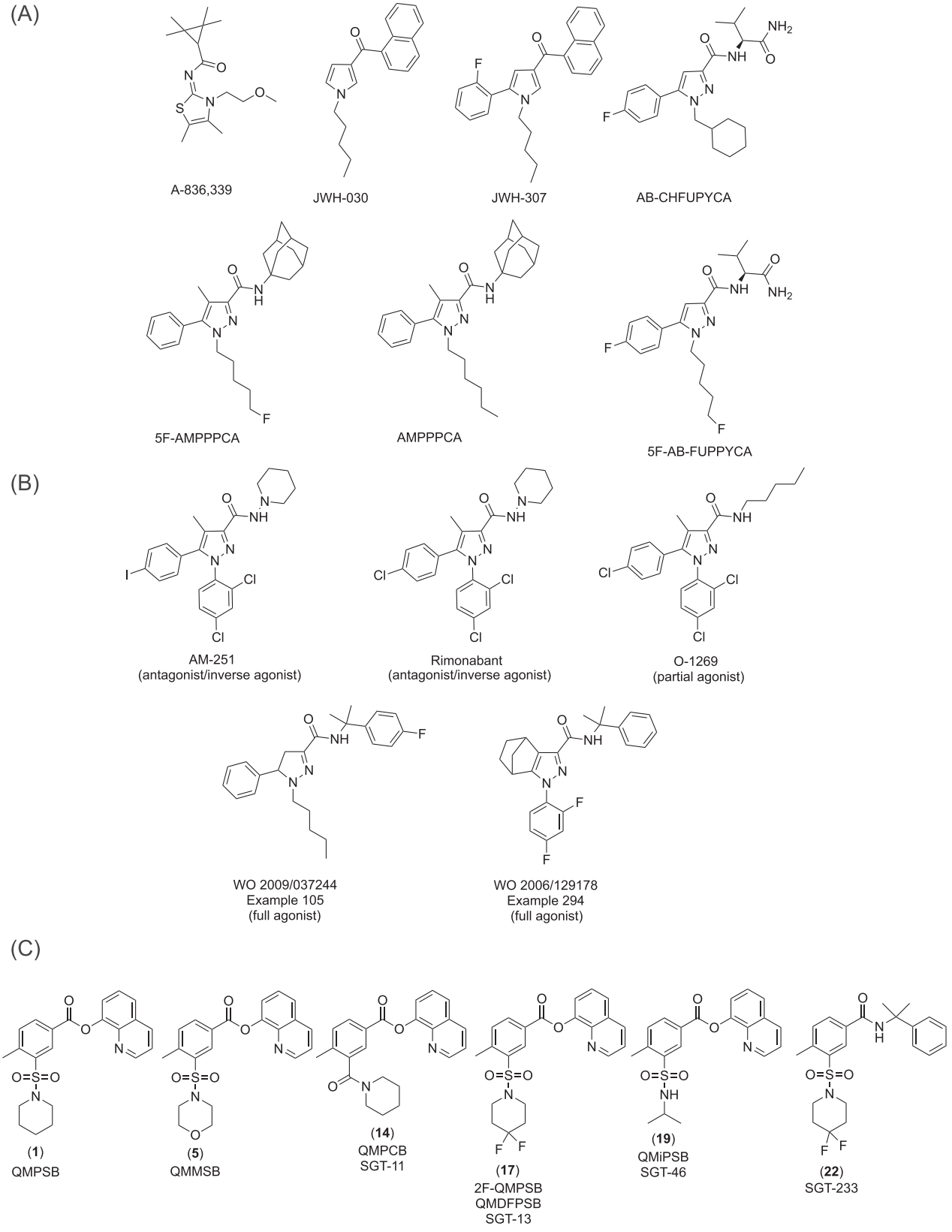

FIGURE 1 A, Examples of synthetic cannabinoid ligands with a monocyclic core that have been detected as new psychoactive substances. B, Additional examples of synthetic cannabinoid ligands containing a pyrazole core with varying functional effects. C, Chemical structures of synthetic cannabinoid receptor agonists QMPSB (**1**), QMMSB (**5**), QMPCB (**14**), 2F-QMPSB (**17**), and QMiPSB (**19**) subjected to analytical characterizations

energy of 70 eV. The ion source temperature was set at 175°C, and the emission current was 50 μA for TSQ 8000 Evo and 400 μA for TSQ 7000. For recording EI-MS, the scan time was 1 s, spanning a scan range between *m/z* 29 and 600, and the samples were injected in the splitless mode. For CI, the reagent gas was methane, and the source pressure was 1.5 mTorr (0.2 Pa). The scan time was 0.5 s, and the scan range was *m/z* 50–600, and the samples were injected in the splitless mode.

In the EI- and CI-MS/MS product ion mode, the scan range under all other identical conditions described earlier started at *m/z* 10 and ended about 10 mass units above the ion that was examined. The collision gas was argon. The collision energy was approximately 20 eV, and the collision gas pressure was approximately 1.5 mTorr (0.2 Pa). The exact target thickness was set using *n*-butylbenzene in the EI-MS mode and adjusting the intensity ratios *m/z* 92/91 to 0.2 and *m/z* 65/91 to 0.02 by varying the collision energy and the collision gas pressure. This method ensured reproducibility of the product ion mass spectra and the use of a product ion mass spectra library for the identification of the structures of the product ions.[30]

The separation was achieved using a fused silica capillary DB-1 column (30 m × 0.25 mm, film thickness 0.25 μm). The temperature program consisted of an initial temperature of 80°C, held for 2 min, followed by an increase to 280°C at 15°C/min. The final temperature was held for 20 min. The injector temperature was 280°C for TSQ 8000 and 220°C for TSQ 7000. The transfer line temperature was set at 280°C, and the carrier gas was helium in constant flow mode at a flow rate of 1.2 mL/min. Retention indices were also determined as Kovats indices calculated from the measurement of an *n*-alkane mixture analyzed with the aforementioned temperature program. Samples were prepared in chloroform.

2.2.2 | Gas chromatography–condensed-phase infrared analysis (GC-sIR)

Samples were also analyzed using a gas chromatography–condensed-phase infrared system (GC-sIR) that consisted of an Agilent GC 7890B (Waldbronn, Germany) with probe sampler Agilent G4567A and a DiscovIR-GC (Spectra Analysis, Marlborough, MA, USA). The column eluate was cryogenically accumulated on a spirally rotating ZnSe disk cooled by liquid nitrogen. IR spectra were recorded through the IR-transparent ZnSe disk using a nitrogen-cooled mercury–cadmium–telluride detector. GC parameters: injection in splitless mode with the injection port temperature set at 240°C and a DB-1 fused silica capillary column (30 m × 0.32 mm i.d., 0.25 μm film thickness). The carrier gas was helium with a flow rate of 2.5 mL/min. The oven temperature program was as follows: 80°C for 2 min, ramped up to 300°C at 20°C/min and held for 22 min. The transfer line was heated at 280°C. Infrared conditions: oven temperature, restrictor temperature, disk temperature, and Dewar cap temperatures were 280°C, 280°C, −40°C, and 35°C, respectively. The vacuum was 0.2 mTorr, disk speed was 3 mm/s, spiral separation was 1 mm, wavelength resolution was 4 cm^{-1}, and IR range was 650–4000 cm^{-1}. Acquisition time was 0.6 s/file with 64 scans/spectrum. Same samples as for mass spectrometric measurements were used. The data were processed using GRAMS/AI Ver. 9.1 (Grams Spectroscopy Software Suite, Thermo Fisher Scientific, Dreieich, Germany) followed by the implementation of the OMNIC Software, Ver. 7.4.127 (Thermo Electron Corporation, Dreieich, Germany). Samples were prepared in chloroform.

2.2.3 | Liquid chromatography–high-resolution mass spectrometry (LC-QTOF-MS/MS)

Quadrupole time-of-flight (QTOF) mass spectra were recorded using an Agilent 6530 QTOF equipped with an Agilent Jet Stream electrospray ionization source and controlled by Agilent MassHunter Acquisition software. The following conditions were used: positive ionization mode, mass range *m/z* 100–1100, collision gas (collision-induced dissociation [CID]) nitrogen, drying gas (N_2) 320°C at 8 L/min, sheath gas 350°C at 11 L/min, nebulizer 35 psi, capillary 3000 V, fragmentor 150 V, nozzle 500 V, skimmer 65 V, collision energy levels between 5.0 and 10.0 V. Accurate mass measurements were obtained through reference correction using protonated purine (*m/z* 121.0509) and protonated HP-921 (*m/z* 922.0098). Data processing was performed using Agilent Masshunter Qualitative software. Separations were performed using a Kinetex C8 column (2.1 × 100 mm, 1.7 μm) (Phenomenex, Aschaffenburg, Germany). Aqueous mobile phase A was water (10 mM ammonium formate, 0.1% formic acid) and mobile phase B was methanol. A gradient elution profile was chosen: 10% B held for 1.5 min, then to 50% B in 7.0 min, followed by an increase to 95% B within 9 min. Flushing and reconditioning were completed by the 11 min mark. The flow rate was 0.275 mL/min, column temperature was 45°C, and the injection volume was 1 μL. The MS/MS spectra were evaluated in two steps. The first step involved using the "find compounds by formula" algorithm to generate averaged MS/MS spectra for each compound (separate MS/MS spectra per collision energy). Isotope signals were then removed. In the following step, the formulae for each fragment peak were generated considering the molecular formula of the precursor ion, and the shown mass was adjusted within the defined range (10 ppm).

2.2.4 | Liquid chromatography–electrospray ionization single quadrupole mass spectrometry (LC-Q-MS)

LC–MS was performed on an Agilent 1100 LC system coupled to a Hewlett Packard/Agilent 1100 MSD (Santa Clara, CA, USA). The following conditions were used: capillary voltage 3500 V, drying gas (N_2) 12 L/min at 350°C, and nebulizer (N_2) pressure 50 psig. The mass spectrometer was tuned according to the manufacturer's instructions using ESI Tuning Mix G2421A (Agilent Technologies).

Separations were performed using a Kinetex F5 column (2.6 μm, 100 Å; 100 × 2.1 mm) (Phenomenex, Macclesfield, UK). Mobile phase A consisted of acetonitrile (containing 0.1% formic acid), and mobile phase B consisted of water (containing 0.1% formic acid). Elution commenced at 6% A (0–2 min), then by a linear gradient up to 30% A at 30 min followed by a linear gradient down to 6% A at 31 min which was held at 6% A for 9 min (run time 40 min). The flow rate was 300 μL/min, and the injection volume was 1 μL.

2.2.5 | Nuclear magnetic resonance spectroscopy (NMR)

Samples were prepared in deuterated dimethyl sulfoxide (DMSO-d_6), and ^{1}H (600 MHz) and ^{13}C DEPTQ (150 MHz) spectra were recorded on a Bruker AVANCE III 600 MHz NMR spectrometer (Coventry, UK). Spectra were referenced to residual solvent, and assignments were supported by 1D and 2D experiments.

3 | RESULTS AND DISCUSSION

3.1 | Chemical analysis

3.1.1 | Electron and chemical ionization mass spectrometry

Electron ionization (EI) and chemical ionization (CI) single (MS) and tandem mass spectra (MS/MS) for all six analytes are shown in Figures 2–4. The EI mass spectrum recorded for QMPSB (**1**) was consistent with the spectrum reported previously,[29] and comparison with the EI mass spectrum of its morpholine analog (**5**) (Figure 4) showed a high similarity apart from some fragments that reflected the mass shift of 2 Da where the methylene unit in the 4′-position of the piperidine ring was replaced by an oxygen atom in the morpholine ring. In both cases, the base peak was detected at *m/z* 263, and as proposed in Figure 5A, its formation was observed independent of the tail group. The remaining four analytes also showed the *m/z* 263 fragment, presumably formed by an equivalent mechanism (supporting information)

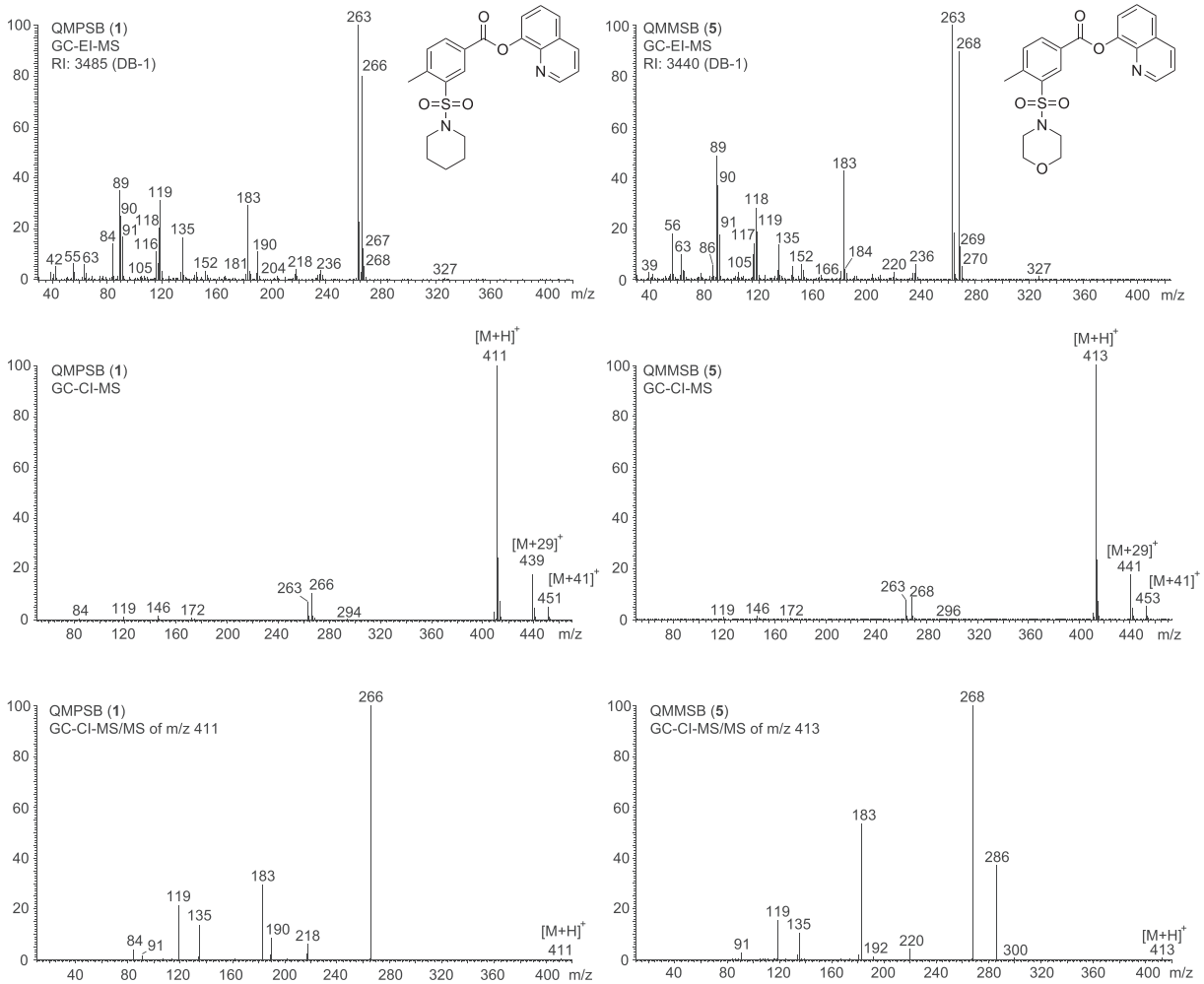

FIGURE 2 Gas chromatography–electron ionization mass spectrometry, gas chromatography–chemical ionization mass spectrometry, and gas chromatography–chemical ionization tandem mass spectrometry data recorded from QMPSB (**1**) and QMMSB (**5**)

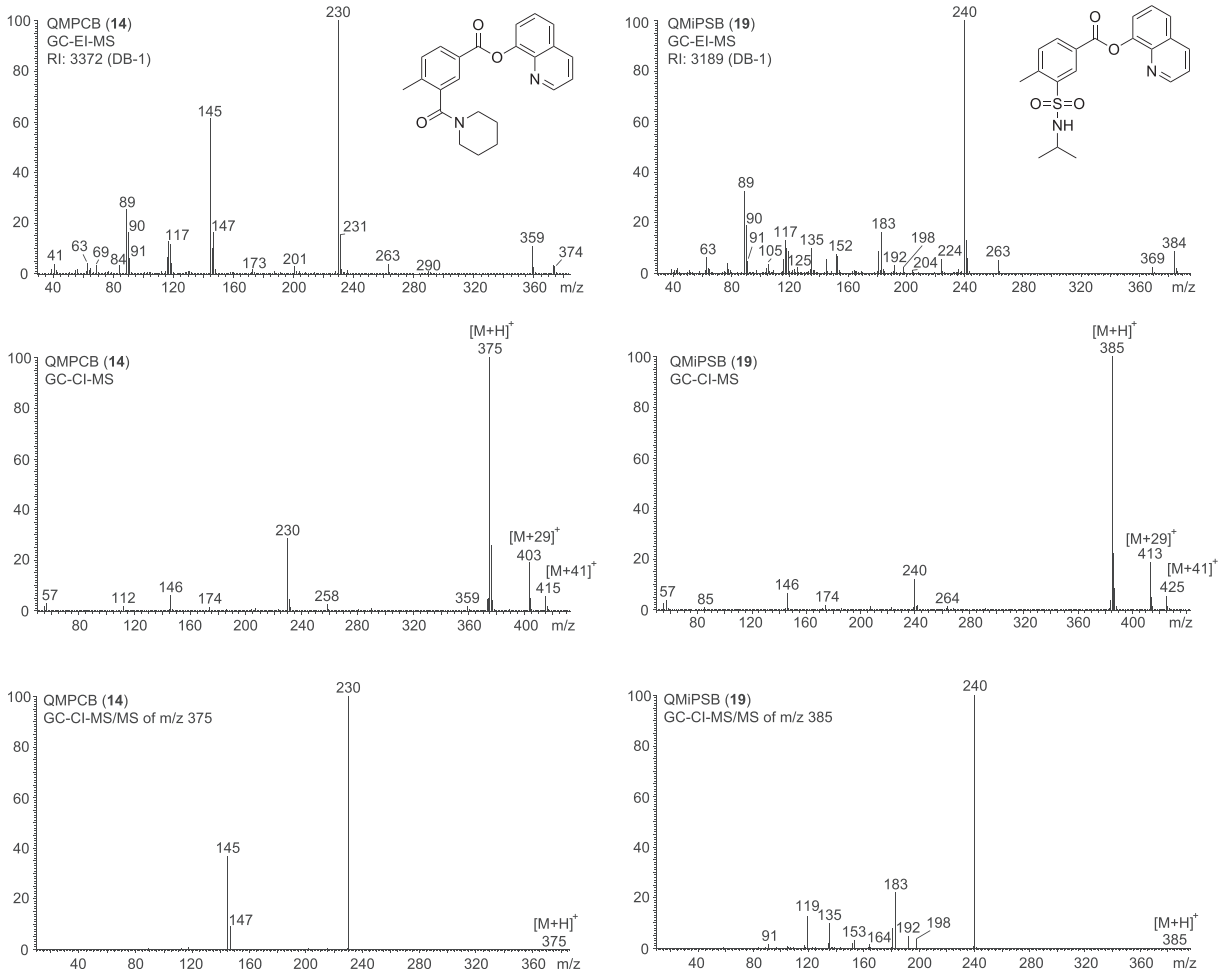

FIGURE 3 Gas chromatography–electron ionization mass spectrometry, gas chromatography–chemical ionization mass spectrometry, and gas chromatography–chemical ionization tandem mass spectrometry data recorded from QMPCB (**14**) and QMiPSB (**19**)

even though it was more pronounced in the EI mass spectrum of 2F-QMPSB (**17**) (Figure 4).

The second most prominent fragment reflected the mass difference between (**1**) and (**5**), thus leading to expected benzoyl ions following α-cleavage (*m/z* 266 in [**1**] and m/z 268 in [**5**]). Correspondingly, the remaining carboxylate analogs (**14**, **17**, and **19**) yielded *m/z* 230, 240, and 302 (supporting information for proposed mechanisms). The cumyl carboxamide SGT-233 (**22**) also generated the same ion at *m/z* 302 ion although its relative abundance was lower compared to the others. In this EI mass spectrum, the base peak was observed at *m/z* 118, possibly reflecting two distinct mechanisms of formation (Figure 5B). A small *m/z* 253 ion might have been formed by a comparable mechanism (supporting information) that yielded *m/z* 263 formed in the mass spectra of the remaining five analytes mentioned earlier. The EI mass spectrum recorded for 2F-QMPSB (**17**) in this investigation was identical to the one published in the public domain that was recorded from standard reference material.[31]

The close structural proximity of most analytes investigated in this study was also reflected in other common fragments such as those found at *m/z* 135 or *m/z* 183 (Figures 2–4) although their identity might not have always been the same (Figure 5A,B). However, these were not detected in the mass spectrum of the *N*-benzoylpiperidine-based QMPCB (**14**). Other ions worth noting included fragment clusters *m/z* 89–91 and *m/z* 116–121 with varying abundance. A proposed fragmentation scheme is shown in Figure 6.

The EI mass spectrum that suggested the presence of a quinolin-8-ol moiety most predominantly was seen in QMPCB (**14**) where the *m/z* 145 ion was the second most abundant peak. As suggested in Figure 7, further fragmentation might have yielded some of the ions found in the fragment clusters.[32] A comparison of all six mass spectra also showed that only three analytes (**14**, **19**, and **22**) displayed a loss of a methyl radical from the molecular ion (Figures 2–4).

The GC–CI-MS(/MS) analysis using methane as the reagent gas provided convenient access to protonated molecules to confirm the mass of the analytes that could not be confirmed in all cases in EI mode (Figures 2–4). Single stage mass analysis alone provided some valuable information due to the generation of some product ions of varying abundance with some being detected under MS/MS conditions with increased abundance (see below). Interestingly, a number of examples showing specific product ions in single stage mode that

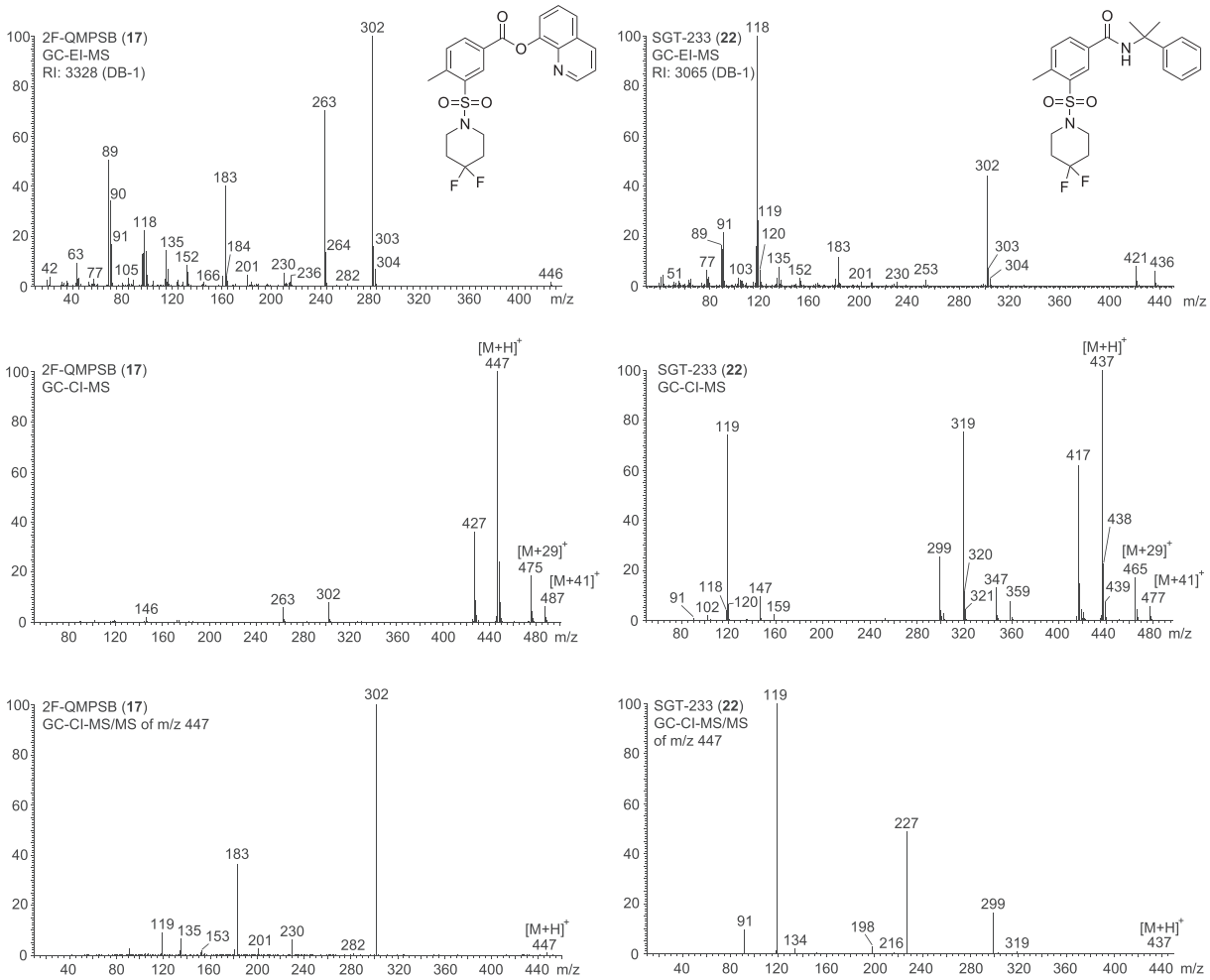

FIGURE 4 Gas chromatography–electron ionization mass spectrometry, gas chromatography–chemical ionization mass spectrometry, and gas chromatography–chemical ionization tandem mass spectrometry data recorded from 2F-QMPSB (**17**) and SGT-233 (**22**)

appeared to be undetectable in the corresponding CI tandem mass spectra presumably reflecting the impact on ion formation related to different collision energies. The two most distinctive examples were observed in the CI mass spectra recorded for the 4′,4′-difluoropiperidines 2F-QMPSB (**17**) and SGT-233 (**22**) (Figure 4). For example, a loss of 20 Da consistent with HF (*m/z* 427 and *m/z* 417) could be seen in single stage but not in the tandem mass spectra. Other differences seen in the CI mass spectrum of SGT-233 (**22**) included *m/z* 347, 359, and a much more prominent *m/z* 319 product ion (Figure 8). Under single stage conditions, the formation of the *m/z* 147 might have involved two separate species including one possibly more typical for EI conditions.[33] Suggestions for the formation of other ions detected under single stage conditions in the remaining spectra are included in the supporting information.

Tandem mass spectral experiments using the protonated molecules as precursor ions also provided valuable insights. Similar to the observation made during the analysis by EI, QMPSB (**1**) and QMMSB (**5**) yielded some identical but also some distinct product ions under CI-MS/MS conditions. The base peaks detected at *m/z* 266 and *m/z* 268 are suggested to be comparable to the benzoyl ions observed during the EI analysis (Figures 2 and 5). Other product ions representing the 2 Da mass differences were detected at *m/z* 190/192 and *m/z* 218/220, which might have indicated a loss of quinoline followed by carbon monoxide (Figure 9). A significant observation was that the CI-MS/MS spectrum of QMMSB (**5**) contained a product ion of appreciable abundance at *m/z* 286 that could be rationalized by the formation of 4-methyl-3-(morpholin-4-ylsulfonyl)benzoic acid (Figure 9), but the corresponding counterpart (mass difference of 2 Da and expected at *m/z* 284) was not detected in the case of QMPSB (**1**). Apart from *N*-benzoylpiperidine-based QMPCB (**14**), common product ions detected in the four remaining sulfamoyl benzoates (**1**, **5**, **17**, and **19**) included *m/z* 91, 119, 135, 183 (Figures 4–6). Proposed mechanisms for product ions formed in the CI tandem mass spectra are included in the supporting information.

3.1.2 | Electrospray ionization mass spectrometry

Electrospray ionization (ESI) MS(/MS) investigations appeared to show some similarities with product ions formed during CI-MS/MS

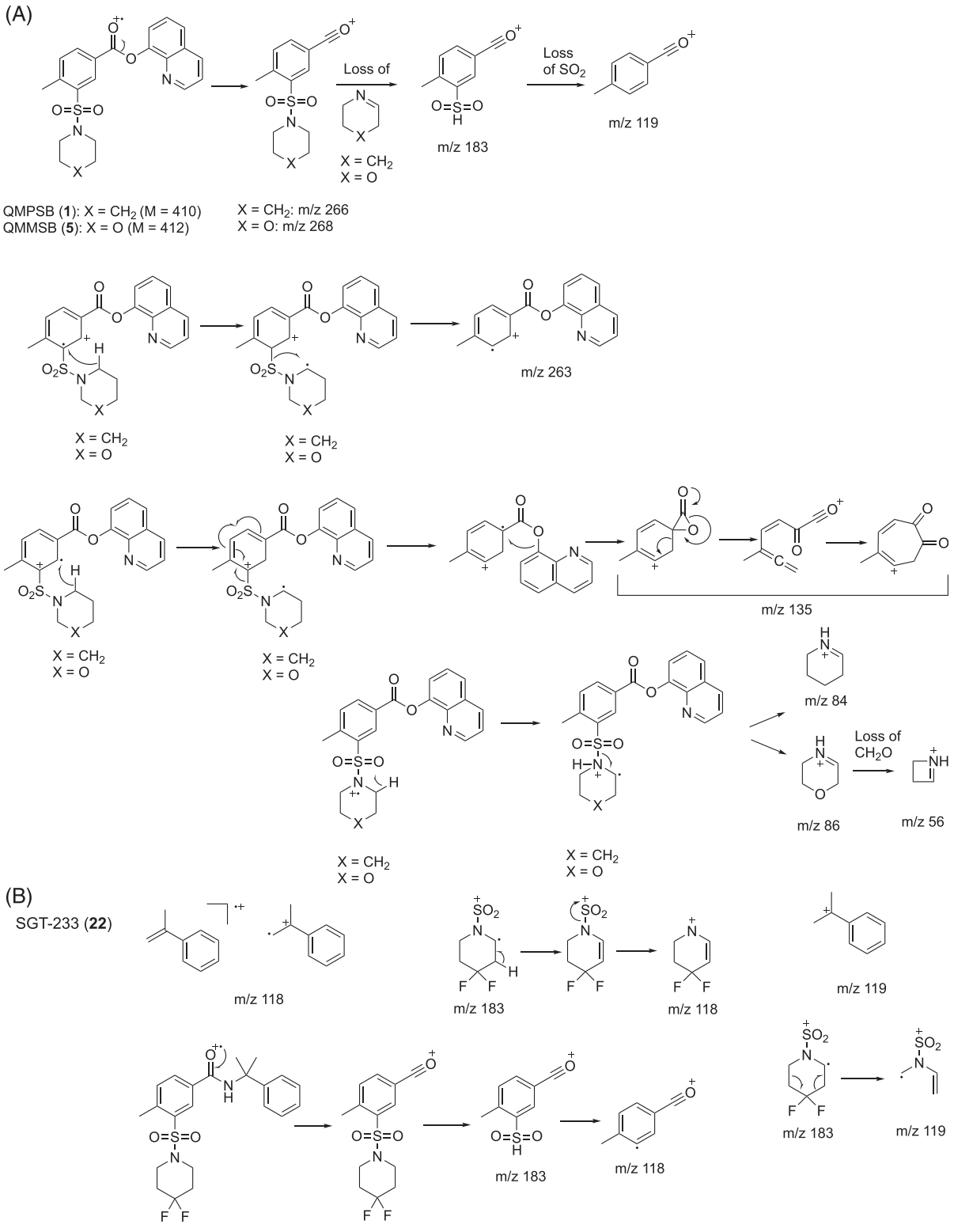

FIGURE 5 A, Proposed electron ionization (EI) mass spectral fragmentation pathways of key ions recorded for QMPSB (**1**) and QMMSB (**5**). B, Proposed formation of *m/z* 119 and *m/z* 118 in the EI mass spectrum of SGT-233 (**22**)

analysis as well. An example is shown in Figure 10, which depicts the QTOF-MS/MS and single quadrupole (Q) mass spectra of QMMSB (**5**) along with proposed identities of product ions. Similar to ions observed under CI-MS/MS conditions (Figure 2), key ions detected following ESI analysis included *m/z* 268, 286 (Q-MS only), 220 (QTOF-MS/MS only), 183, 135, and 119 (Figure 10). The proposed fragmentation pathways were comparable to those suggested earlier (CI-MS/MS, Figure 9) but with the additional support of exact

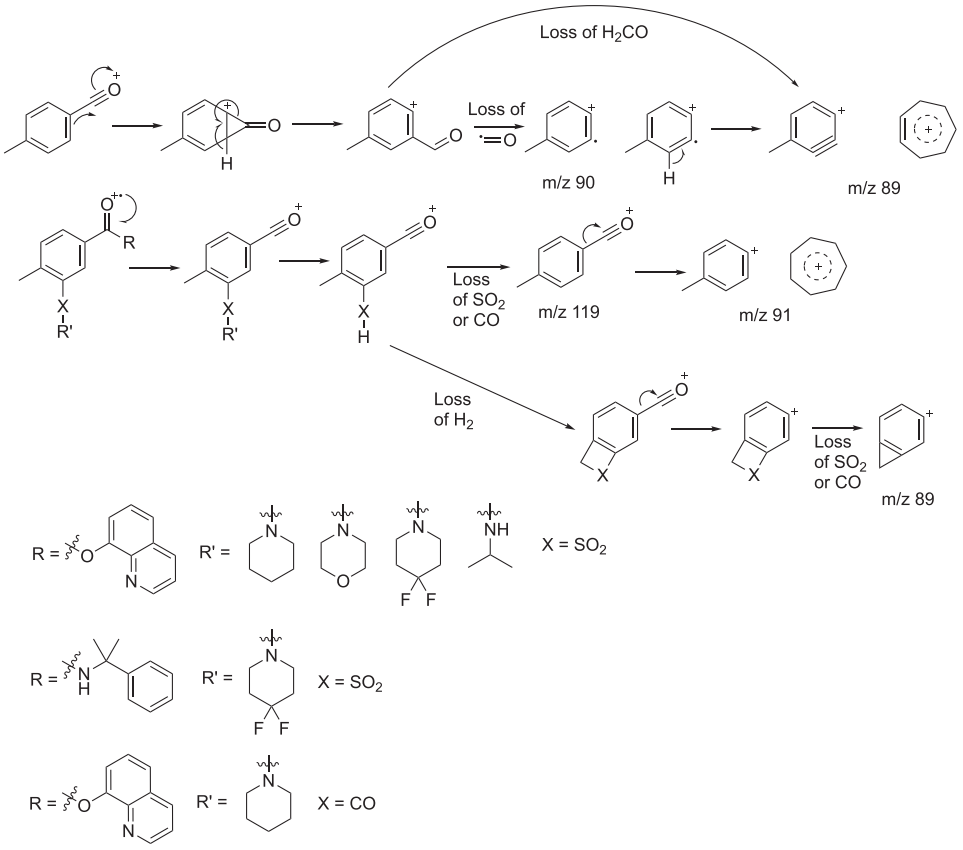

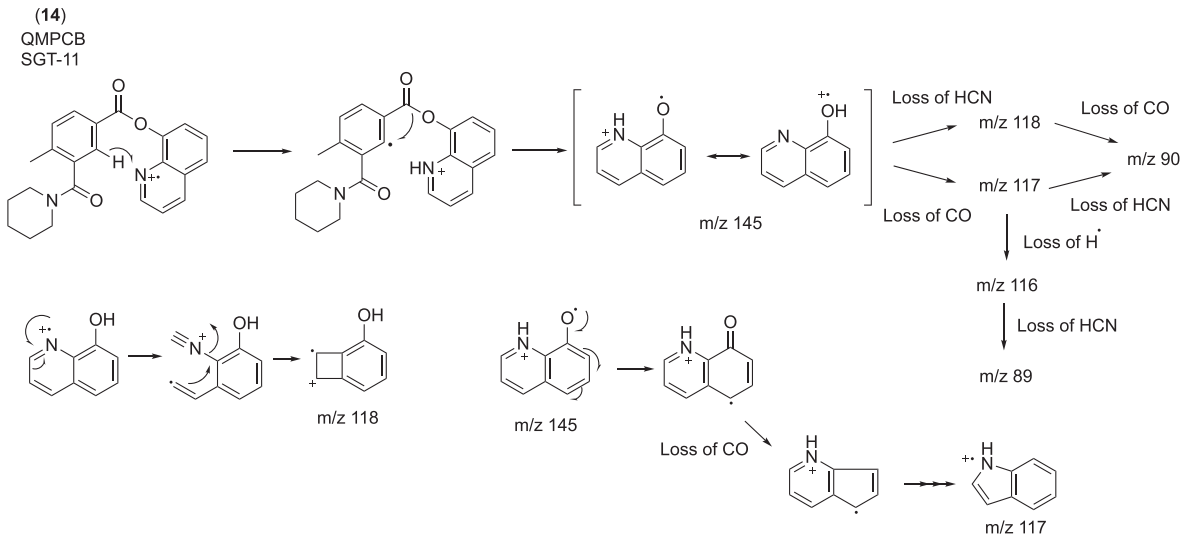

FIGURE 6 Proposed electron ionization mass spectrometry fragmentation pathways that might account for the formations of *m/z* 89, 90, and 91

FIGURE 7 Proposed electron ionization mass spectrometry fragmentation pathway associated with the quinolin-8-ol moiety

mass measurements, with the benzoyl ion at *m/z* 268.0629 ($C_{12}H_{14}NO_4S^+$, Δ = −3.36 ppm) forming the base peak. The product ions at *m/z* 183, 135, 119, and 91 were also detected in the QqQ-MS/MS investigations published on the characterization of QMPSB (**1**) with the main difference associated with the mass shift of 2 Da that yielded the benzoyl ion base peak at *m/z* 266.[29] The remaining ESI high-resolution mass spectra can be found in the supporting information.

3.1.3 | Spectroscopic features

The nuclear magnetic resonance (NMR) spectroscopy data for all six SCRAs are summarized in Table 1 with full 1D and 2D spectra shown in the supporting information. For consistency with the reported data, the numbering scheme was adopted from Blakey and coworkers who reported the analytical characterization of QMPSB (**1**).[29] Assignments were aided by 1D and 2D experiments,

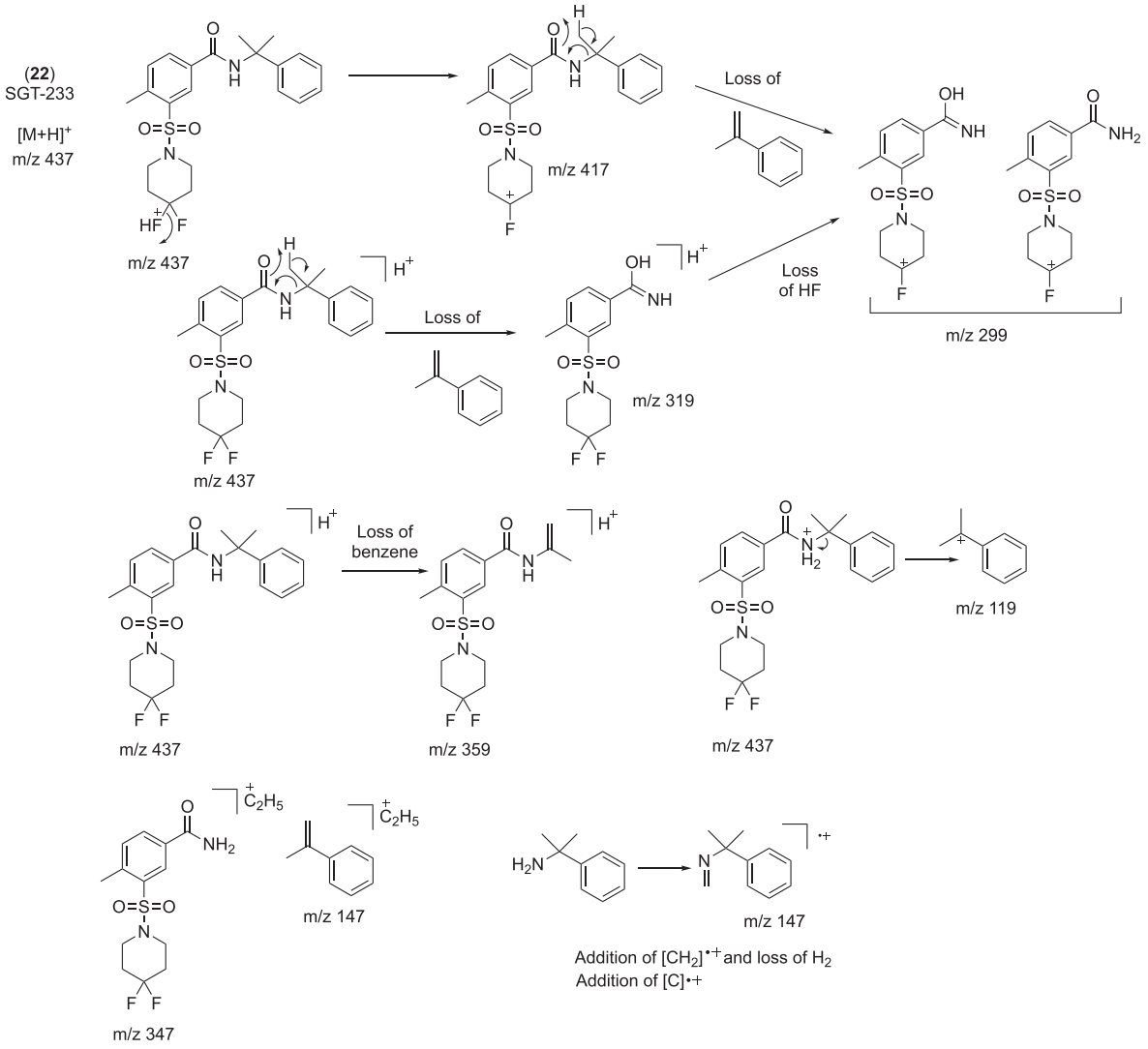

FIGURE 8 Proposed chemical ionization mass spectrometry fragmentation pathway of SGT-233 (**22**)

and the spectral data recorded for QMPSB (**1**) in this study were consistent with the data reported for the same compound in both $CDCl_3$ (Table 1) and DMSO-d_6 (supporting information).[29] In QMPSB (**1**), and similar to representatives such as 1-[(2-methylphenyl)sulfonyl]piperidine,[34] protons and carbons belonging to the piperidine ring were detected as three distinct resonances with the 2′/6′-related signals being shifted more downfield than 3′/5′ and 4′, respectively. The same was observed with 2F-QMPSB (**17**) and SGT-233 (**22**), which contained the 4′,4′-difluoropiperidine moiety though the presence of the fluorine atoms led to a more downfield shift of 3′/5′ resonances. Correspondingly, the carbon spectra for these two substances showed three triplets for C-4′, C-3′/5′, and C-2′/6′ due to carbon–fluorine coupling (Table 1). In the case of the morpholine analog QMMSB (**5**), the order was reversed where the 3′/5′ protons and carbons shifted significantly more downfield similar to spectral data reported for 4-[(2-methylphenyl)sulfonyl]morpholine.[35] However, in QMPCP (**14**), the presence of a *N*-benzoylpiperidine motif resulted in the multiplication of resonances due to restricted rotation induced around the amide bond. Similar to what was observed for *N*-benzoylpiperidine itself, carbon resonances of C-2′/6′ (α to *N*) and C-3/5′ (β to *N*) were observed as four distinct signals[36,37] in addition to one resonance more upfield reflecting C-4′ (Table 1). QMPCP (**14**) showed two multiplets of two protons for H-2′/6′, whereas a broad singlet integrating into four protons was observed for H-3′/5′ consistent with *N*-benzoylpiperidine and derivatives.[37] The order of proton and carbon chemical shifts observed for the quinolin-8-yl moieties in QMPSB (**1**), QMMSB (**5**), and 2F-QMPSB (**17**) was almost identical to those reported for other SCRAs carrying this head group such as PB-22 (**27**)[38] and quinolin-8-yl-1-(5-fluoropentyl)-1*H*-pyrrolo[2,3-*b*]pyridine-3-carboxylate (5F-NPB-22-7N, 7N-5F-PB-22)[39] which were also recorded in $CDCl_3$.

All GC-sIR spectra recorded from the six compounds are included in the supporting information, and the spectrum recorded for QMPSB (**1**) appeared comparable to the one published by

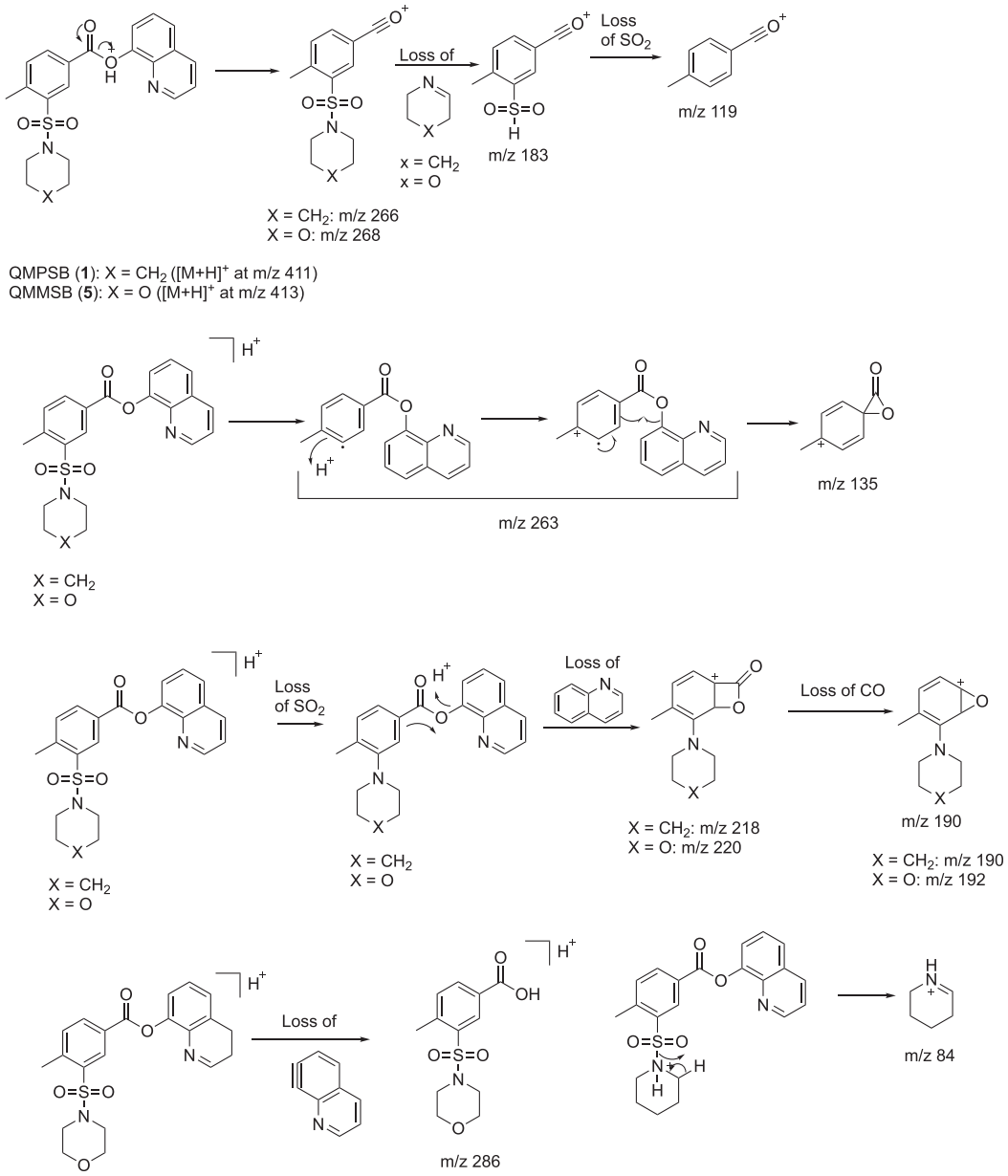

FIGURE 9 Proposed chemical ionization tandem mass spectrometry fragmentation pathways of key ions of QMPSB (**1**) and QMMSB (**5**)

Blakey and colleagues.[29] Apart from the cumyl derivative SGT-233 (**22**), all remaining spectra recorded showed the ester-based carbonyl band between 1741 and 1745 cm^{-1}. QMPCB (**14**), the amide analog of QMPSB (**1**), displayed an amide band at 1633 cm^{-1}, whereas the cumyl carboxamide head group in SGT-233 (**22**) exhibited its amide stretch at 1670 cm^{-1}. The bands associated with the NH amide stretches present in QMiPSB (**19**) and SGT-233 (**22**) were detected at 3286 and 3374 cm^{-1}. Additional suggested assignments can be found in the supporting information.[40] Under the GC-sIR conditions used, eluting analytes deposited cryogenically onto an IR-transparent zinc selenide disk, which enabled the collection of IR spectra of a solidified eluent, thus making it comparable to those recorded under traditional ATR-IR conditions.

3.2 | Detection of impurities

Analyses of all six analytes by GC–MS showed the presence of various impurities (supporting information) as indicated by the detection of additional peaks. Except sulfamoyl benzamide SGT-233 (**22**), the GC–MS traces of other analytes showed the presence of quinolin-8-ol (8-hydroxyquinoline) as a reflection of the quinolin-8-yl ester head group. However, whether it was present in the sample or artificially induced during GC–MS analysis was not clear, a phenomenon commonly observed with such esters (unpublished observation). Examples reported in the literature include quinolin-8-ol detection during the analysis of quinolin-8-yl-1-pentyl-1*H*-indole-3-carboxylate (PB-22, **28**)[41,42] and QMPSB (**1**)[29] as a reflection of thermal degradation.

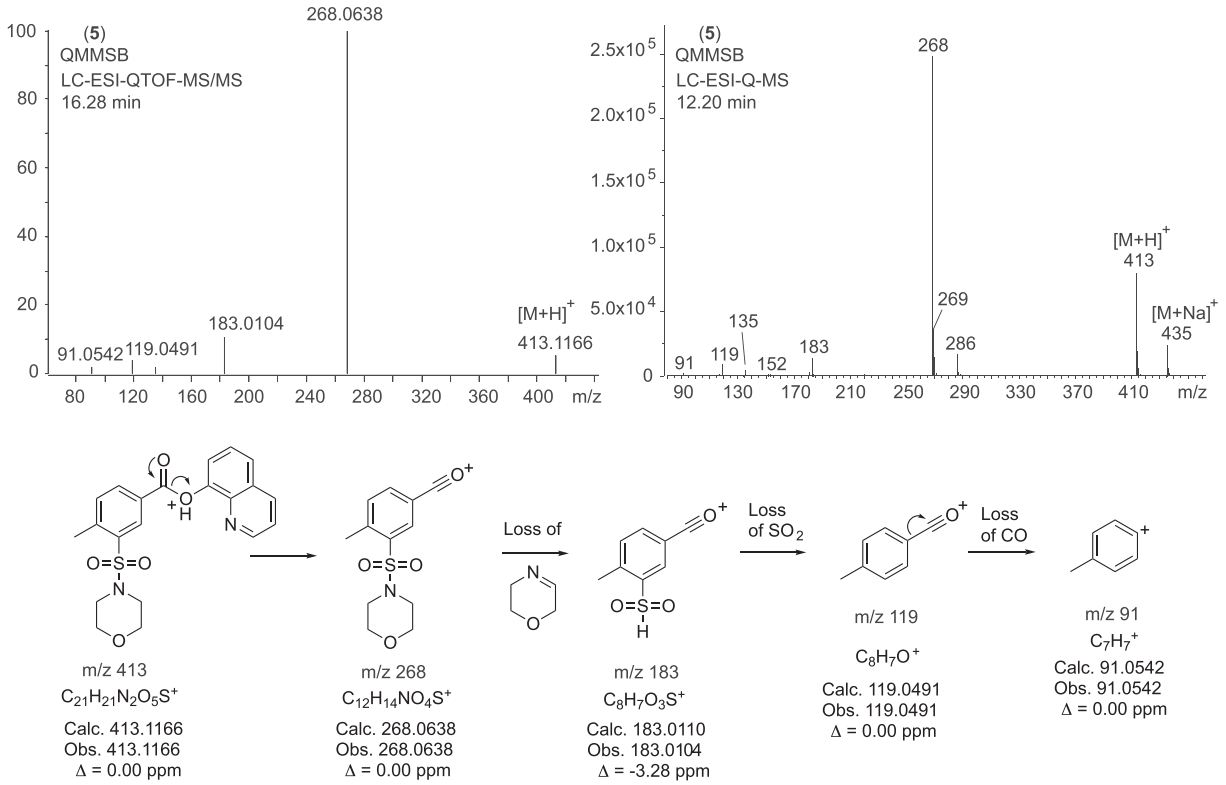

FIGURE 10 Electrospray ionization–quadrupole time-of-flight tandem mass spectrometry and electrospray ionization–single quadrupole mass spectrometry data and proposed fragmentation pathways related to QMMSB (**5**)

Also except SGT-233 (**22**), the GC–MS traces of other analytes showed the presence of an ethyl ester impurity (supporting information), consistent with what was reported during the analysis of QMPSB (**1**) where *trans*-esterification was observed as a consequence of employing methanol and ethanol during the sample preparation procedure that was avoided when using dichloromethane.[29] In this study, chloroform was used when dissolving the samples for GC–MS analysis. Whether traces of ethanol were present from unrelated work during previous injections could not be determined with certainty but seemed possible. The presence of ethanol as a stabilizing agent in the chloroform solvent might also account for this observation.

However, analysis of the morpholine analog QMMSB (**5**) revealed the identification of the ethyl ester impurity that could subsequently be isolated by preparative thin-layer chromatography (TLC) (silica gel, 0.5 mm; mobile phase EtOAc/hexane, 8/2, v/v, extracted with EtOAc), thus confirming that this was present in the sample. The GC–MS trace and the EI mass spectrum are shown in Figure 11A together with a proposed fragmentation scheme that seemed consistent with its structure. For example, the molecular ion was detected at *m/z* 313, and the base peak at *m/z* 86 was consistent with the unsaturated morpholine fragment that subsequently might have undergone ring contraction via the neutral loss of formaldehyde to give *m/z* 56. Various other ions were comparable to those also detected in the EI mass spectrum of QMMSB (**5**) (Figure 2). The EI mass spectrum also showed several similarities with the spectrum recorded for the ethyl ester counterpart of QMPSB (**1**) published previously with some fragments exhibiting the 2 Da mass shift as expected, such as *m/z* 84, *m/z* 266, and *m/z* 311 for the molecular ion.[29]

Given that the ethyl ester impurity was not solely detected as a GC-induced artifact, its detection was therefore also feasible by LC-Q-MS as shown in Figure 11B where it was observed in the full scan mode. Under LC-Q-MS conditions, the protonated molecule was detected at *m/z* 314 in addition to a sodiated adduct at *m/z* 336.

The presence of the ethyl ester was also reflected in the NMR spectra recorded for the impure mixture consisting of QMMSB (**5**) and the ethyl ester impurity (supporting information). Following isolation by preparative TLC, analysis by NMR (full spectra in the supporting information) showed that the spectral data were consistent with its structure: ^{1}H NMR (600 MHz, $CDCl_3$) δ 8.53 (d, J = 1.8 Hz, 1H, H-2), 8.13 (dd, J = 7.9, 1.8 Hz, 1H, H-6), 7.42 (d, J = 7.9 Hz, 1H, H-5), 4.40 (q, J = 7.1 Hz, 2H, OCH_2), 3.77–3.65 (m, 4H, H-3′/5′), 3.25–3.14 (m, 4H, H-2′/6′), 2.70 (s, 3H, 4-CH_3), 1.41 (t, J = 7.1 Hz, 3H, CH_3); ^{13}C NMR (150 MHz, $CDCl_3$) δ 165.11 (C=O), 143.12 (C-4), 135.94 (C-3), 133.73 (C-6), 133.17 (C-5), 131.23 (C-2), 128.99 (C-1), 66.34 (C-3′/5′), 61.54 (OCH_2), 45.39 (C-2′/6′), 21.06 (4-CH_3), 14.33 (CH_3).

As shown in the supporting information, GC–MS analysis of the two 4′,4′-difluoropiperidines SGT-233 (**22**) and 2F-QMPSB (**17**) also showed another chromatographic peak with EI mass spectra reflecting what might have been consistent with a loss of HF from the molecule. The EI mass spectra of the two 4-fluoro-

TABLE 1 Nuclear magnetic resonance data recorded in $CDCl_3$ (600/150 MHz).

	QMPSB (1)		QMMSB (5)		QMPCP (14)	
	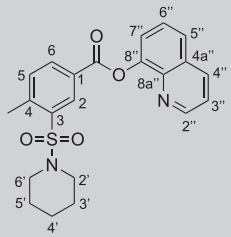		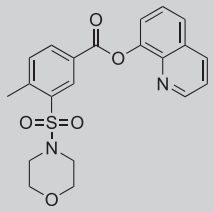		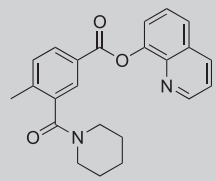	
Position	**^{1}H**	**^{13}C**	**^{1}H**	**^{13}C**	**^{1}H**	**^{13}C**
1	–	127.86	–	128.13		127.48
2	8.82 (d, *J* = 1.7 Hz, 1H)	131.79	8.83 (d, *J* = 1.7 Hz, 1H)	132.09	8.14 (s, 1H)	128.05
3	–	137.67	–	136.45	–	137.22
4	–	143.89	–	143.94	–	140.56
4-CH_3	2.76 (s, 3H)	21.03	2.77 (s, 3H)	21.19	2.43 (s, 3H)	19.45
5	7.50 (d, *J* = 7.9 Hz, 1H)	133.19	7.53 (d, *J* = 7.9 Hz, 1H)	133.41	7.39 (d, *J* = 7.9 Hz, 1H)	130.71 or 130.74
6	8.39 (dd, *J* = 7.9, 1.8 Hz, 1H)	134.15	8.42 (dd, *J* = 7.9, 1.8 Hz, 1H)	134.60	8.24 (d, *J* = 8.0 Hz, 1H)	130.71 or 130.74
1″	–	–	–	–	–	–
2″	8.88 (dd, *J* = 4.2, 1.6 Hz, 1H)	150.60	8.88 (dd, *J* = 4.2, 1.6 Hz, 1H)	150.61	8.89 (d, *J* = 4.0 Hz, 1H)	150.57
3″	7.44 (dd, *J* = 8.3, 4.2 Hz, 1H)	121.82	7.45 (dd, *J* = 8.3, 4.2 Hz, 1H)	121.85	7.43 (dd, *J* = 8.2, 4.2 Hz, 1H)	121.75
4″	8.22 (dd, *J* = 8.3, 1.6 Hz, 1H)	136.05	8.22 (dd, *J* = 8.3, 1.6 Hz, 1H)	136.05	8.20 (d, *J* = 8.3 Hz, 1H)	136.03
4a″	–	129.64	–	129.64	–	129.61
5″	7.79 (dd, *J* = 7.8, 1.7 Hz, 1H)	126.27 or 126.24	7.79 (dd, *J* = 7.7, 1.8 Hz, 1H)	126.29 or 126.26	7.77 (d, *J* = 7.9 Hz, 1H)	126.04
6″	7.62–7.55 (m, 1H)	126.27 or 126.24	7.62–7.56 (m, 1H)	126.29 or 126.26	7.61–7.53 (m, 1H)	126.28
7″	7.62–7.55 (m, 1H)	121.56	7.62–7.56 (m, 1H)	121.50	7.61–7.53 (m, 1H)	121.66
8″	–	147.51	–	147.46	–	147.68
8a″	–	141.25	–	141.18	–	141.38
2′	3.28–3.22 (m, 2H)	46.20	3.31–3.22 (m, 2H)	45.47	3.82–3.71 (m, 2H) 3.30–3.21 (m, 2H)	42.55 48.05
3′	1.68–1.61 (m, 2H)	25.49	3.79–3.72 (m, 2H)	66.39	2 H from 1.71–1.64 (m, 4H)	25.70 24.53
4′	1.53–1.58 (m, 2H)	23.79	–	–	1.59–1.44 (m, 2H)	26.62
5′	1.68–1.61 (m, 2H)	25.49	3.79–3.72 (m, 2H)	66.39	2 H from 1.71–1.64 (m, 4H)	25.70 24.53
6′	3.28–3.22 (m, 2H)	46.20	3.31–3.22 (m, 2H)	45.47	3.82–3.71 (m, 2H) 3.30–3.21 (m, 2H)	42.55 48.05
C=O (ester)	–	164.21	164.01		–	164.93
C=O (amide)	–	–	–	–	–	168.72
NH	–	–	–	–	–	–
CH	–	–	–	–	–	–
2 × CH_3	–	–	–	–	–	–
C_{quat}	–	–	–	–	–	–

Abbreviations: 2F-QMPSB, quinolin-8-yl 3-(4,4-difluoropiperidine-1-sulfonyl)-4-methylbenzoate; QMMSB, quinolin-8-yl 4-methyl-3-(morpholine-4-sulfonyl)benzoate; QMPCB, quinolin-8-yl 4-methyl-3-(piperidine-1-carbonyl)benzoate; QMPSB, quinolin-8-yl 4-methyl-3-(piperidine-1-sulfonyl)benzoate; QMDFPSB, quinolin-8-yl 3-(4,4-difluoropiperidine-1-sulfonyl)-4-methylbenzoate; SGT-233, 3-(4,4-difluoropiperidine-1-sulfonyl)-4-methyl-*N*-(2-phenylpropan-2-yl)benzamide

(Continues)

TABLE 1 Continued

	bQMDFPSB (17)		2F-QMPSB (19)		SGT-233 (22)	
	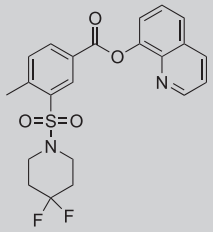		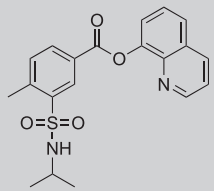		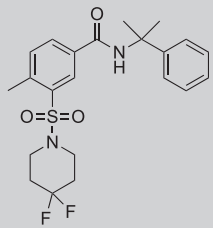	
Position	**^{1}H**	**^{13}C**	**^{1}H**	**^{13}C**	**^{1}H**	**^{13}C**
1	–	128.16	–	129.65	–	133.78
2	8.83 (d, *J* = 1.2 Hz, 1H)	131.68	8.94 (d, *J* = 1.5 Hz, 1H)	131.14	8.27 (d, *J* = 1.8 Hz, 1H)	128.10
3	–	137.40	–	139.88	–	136.78
4	–	143.68	–	142.93	–	141.22
4-CH_3	2.74 (s, 3H)	20.88	2.78 (s, 3H)	20.67	2.64 (s, 3H)	20.49
5	7.53 (d, *J* = 7.8 Hz, 1H)	133.42	7.50 (d, *J* = 7.9 Hz, 1H)	132.99	7.39 (d, *J* = 7.9 Hz, 1H)	133.33
6	8.42 (dd, *J* = 7.8, 1.3 Hz, 1H)	134.64	8.40 (dd, *J* = 7.8, 1.7 Hz, 1H)	134.24	7.87 (dd, *J* = 7.9, 1.9 Hz, 1H)	131.48
1″	–	–	–	–	–	146.41
2″	8.88 (dd, *J* = 4.0, 0.9 Hz, 1H)	150.62	8.89 (dd, *J* = 4.1, 1.4 Hz, 1H)	150.60	7.45 (dd, *J* = 8.4, 1.1 Hz, 1H)	124.71
3″	7.45 (dd, *J* = 8.3, 4.2 Hz, 1H)	121.86	7.45 (dd, *J* = 8.3, 4.2 Hz, 1H)	121.83	7.38–7.33 (m, 1H)	128.58
4″	8.22 (d, *J* = 7.6 Hz, 1H)	136.09	8.22 (dd, *J* = 8.3, 1.4 Hz, 1H)	136.11	7.29–7.23 (m, 1H) * coalescing with solvent	126.95
4a″	–	129.65	–	129.65	–	–
5″	7.79 (dd, *J* = 7.8, 1.2 Hz, 1H)	126.32 or 126.28	7.79 (dd, *J* = 7.8, 1.5 Hz, 1H)	126.29 or 126.26	7.38–7.33 (m, 1H)	128.58
6″	7.63–7.56 (m, 1H)	126.32 or 126.28	7.62–7.55 (m, 1H)	126.29 or 126.26	7.45 (dd, *J* = 8.4, 1.1 Hz, 1H)	124.71
7″	7.63–7.56 (m, 1H)	121.52	7.62–7.55 (m, 1H)	121.59	–	–
8″	–	147.43	–	147.49	–	–
8a″	–	141.16	–	141.19	–	–
2′	3.50–3.44 (m, 2H)	42.70 (t, J_{CF} = 5.6 Hz)	–	–	3.43–3.36 (m, 2H)	42.55 (t, J_{CF} = 5.6 Hz)
3′	2.11 (tt, *J* = 13.0, 5.8 Hz, 2H)	33.98 (t, J_{CF} = 23.7 Hz)	–	–	2.08 (tt, *J* = 13.4, 5.8 Hz, 2H)	33.92 (t, J_{CF} = 23.8 Hz)
4′	–	121.01 (t, J_{CF} = 242.3 Hz)	–	–	–	120.94 (t, J_{CF} = 242.5 Hz)
5′	2.11 (tt, *J* = 13.0, 5.8 Hz, 2H)	33.98 (t, J_{CF} = 23.7 Hz)	–	–	2.08 (tt, *J* = 13.4, 5.8 Hz, 2H)	33.92 (t, J_{CF} = 23.8 Hz)
6′	3.50–3.44 (m, 2H)	42.70 (t, J_{CF} = 5.6 Hz)	–	–	3.43–3.36 (m, 2H)	42.55 (t, J_{CF} = 5.6 Hz)
C=O (ester)	–	164.00	–	164.21	–	164.57
C=O (amide)	–	–	–	–	–	–
NH	–	–	4.41 (d, *J* = 7.9 Hz, 1H)	–	6.41 (s, 1H)	–
CH	–	–	3.63–3.53 (m, 1H) 3.58 (dsept, *J* = 8.0, 6.5 Hz, 1H)	46.32	–	–
2 × CH_3	–	–	1.16 (d, *J* = 6.5 Hz, 6H)	23.94	1.83 (s, 6H)	29.13
C_{quat}	–	–	–	–	–	56.63

Abbreviations: 2F-QMPSB, quinolin-8-yl 3-(4,4-difluoropiperidine-1-sulfonyl)-4-methylbenzoate; QMMSB, quinolin-8-yl 4-methyl-3-(morpholine-4-sulfonyl)benzoate; QMPCB, quinolin-8-yl 4-methyl-3-(piperidine-1-carbonyl)benzoate; QMPSB, quinolin-8-yl 4-methyl-3-(piperidine-1-sulfonyl)benzoate; QMDFPSB, quinolin-8-yl 3-(4,4-difluoropiperidine-1-sulfonyl)-4-methylbenzoate; SGT-233, 3-(4,4-difluoropiperidine-1-sulfonyl)-4-methyl-*N*-(2-phenylpropan-2-yl)benzamide

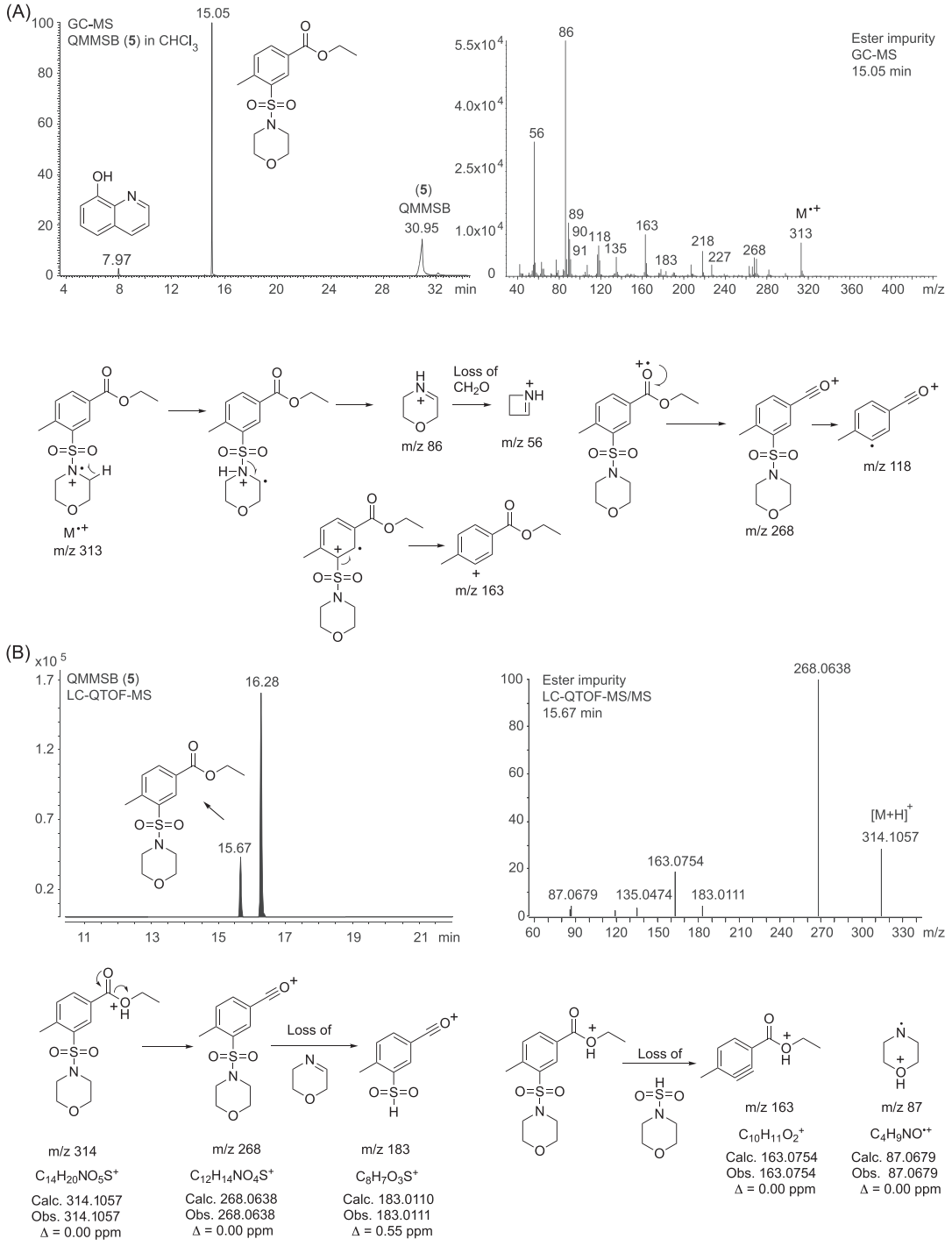

FIGURE 11 Detection of ethyl 4-methyl-3-(morpholin-4-ylsulfonyl)benzoate in QMMSB (**5**). A, Gas chromatography–electron ionization mass spectrometry trace and electron ionization mass spectrum. B, Liquid chromatography–electrospray ionization single quadrupole mass spectrometry trace and mass spectrum induced by in-source collision-induced dissociation and proposed fragmentation pathway for the ester impurity. For nuclear magnetic resonance data of the isolated impurity, see text and the supporting information

1,2,3,6-tetrahydropyridine analogs seemed consistent with the proposed structure. Indications that these detections were not limited to the artificial formation during GC analysis alone came from the inspection of the LC-Q-MS traces that suggested detections of chromatographic peaks associated with protonated molecules at *m/z* 417 (SGT-233 (**22**)–HF) and *m/z* 427 (2F-QMPSB (**17**)–HF). Product ion formations following in-source CID were consistent with this specific modification at the tail group following the mechanism discussed earlier, that is, amide formation at *m/z* 299 for the former and benzoyl ion formation at *m/z* 282 for the latter. However, the LC-Q-MS trace following the analysis of 2F-QMPSB (**17**) also revealed an additional peak with an associated protonated molecule

at *m/z* 429 and suspected benzoyl ion at *m/z* 284. This particular mass difference indicated that this might have represented an impurity carrying a 4-fluoropiperidine moiety on the tail. LC-QTOF-MS data have also been included (supporting information).

3.3 | Historical perspective

QMPSB (**1**) represented a template involving a sulfamoyl benzoate scaffold that was featured in the scientific literature. In 2005[43] (followed by an international patent application in 2006[44]), a patent filed by the Adolor Corporation in the United States of America described the preparation of various sulfamoyl benzamides aimed at the development of CB_2 receptor (CB_2R) selective drugs such as (**2**) (Figure 12), which has initially been found to display a modest binding affinity for CB_2R (CB_1 K_i > 1000 nM, CB_2 K_i = 800 nM).[45,46] Subsequent modifications produced a range of structures with varying CB_1R/CB_2R selectivity including example (**3**) (Figure 12) (CB_1 K_i = 130 nM, CB_2 K_i = 3.9 nM, EC_{50} = 4.6 nM [[^{35}S]GTPγS binding assay][46]). Small changes in the sulfamoyl group were also reported to result in a switch from full agonist to inverse agonist activity[45] and reversal of the amide linkage in (**3**) yielded (**4**) with improved selectivity in binding (CB_1 K_i = 640 nM, CB_2 K_i = 1.7 nM, CB_2EC_{50} = 9.6 nM).[46]

In 2007, Lambeng and coworkers published the identification of the sulfamoyl benzoate QMPSB (**1**) as part of high-throughput screening of their sample collection. It was identified as a potent CB_1R agonist (CB_1 IC_{50} = 0.79 nM, EC_{50} = 10 nM) with moderate selectivity (CB_2 K_i = 25.15 nM).[47] Compound (**1**) was subsequently confirmed to show a high binding affinity for both receptor subtypes (CB_1 K_i = 3 nM; CB_2 K_i = 4 nM) and full agonist properties (cAMP assay) at CB_2R but without selectivity.[48] A range of modifications of lead (**1**) were tested by Lambeng et al., and the structural modifications also included a change from the ester to an amide linker that led to a significant loss of potency.[47] Even though all candidates retaining the ester linker tested were less potent than (**1**) in a functional assay (CB_1R pEC_{50} = 8.0), three substances retained CB_1R pEC_{50} values above 7 (EC_{50} < 100 nM), that is, 7.9, 7.3, and 7.2, respectively, for the morpholine analogs (**5**) (QMMSB), (**6**), and (**7**) (Figures 1A and 13).[47] QMMSB (**5**) was also reported to show an IC_{50} value of 1.26 nM[47] and K_i values of 52.4 and 67.5 nM for hCB_1R.[52] Reports from human volunteers collected during investigations by Stargate International in 2012 suggested (**1**) and (**5**) to be psychoactive and of short duration although both compounds were also found to show relatively poor solubility and thermal instability.

Selectivity toward CB_2R has been investigated further by Ermann and colleagues[48] who extended the evaluation of analogs by switching from the ester linker to an amide, which markedly increased the CB_2 selectivity. However, three compounds still retained significant efficacy at CB_1 (EC_{50} values of 28, 25, and 10 nM at CB_1 and 4, 1, and 5 nM at CB_2 for (**8**), (**9**), and (**10**), respectively.[48] Compound (**11**) was also found that showed a 10-fold selectivity for CB_1R despite lower potency overall (EC_{50} = 228 nM at CB_1R and 2284 nM at CB_2R). Replacing the linker with a heterocycle, such as a 2*H*-tetrazole unit, was also tolerated, as seen, for example, in (**12**) (K_i = 130 nM, EC_{50} = 372 at CB_1; K_i = 17 nM, EC_{50} = 49 nM at CB_2).[46] Unconfirmed reports suggested that analog (**13**) (CBD-003) was under development by European SCRA researchers with claims on psychoactivity, but it is unclear whether this ever emerged as an NPS on the market.

This series of papers and patents established some of the structure–activity relationships for this class of compounds, which, starting in 2012, also triggered interest from Stargate International (SGT) to carry out further research into this class of compounds, with synthesis conducted under contract basis in China. Two novel compounds derived from QMPSB (**1**), which explored the potential for increased potency and CB_1R selectivity. One led to the evaluation of the amide analog QMPCB (SGT-11) (**14**) (Figure 1C), where the sulfonyl group was replaced by carbonyl, in an attempt to assess the importance of the sulfamoyl tail group linker. This modification did not appear to have been covered in the existing literature. Reportedly, this compound retained activity in human volunteers but was reduced in potency compared to QMPSB (**1**) consistent with more recent research showing a carbonyl linker on the tail group to retain high CB binding affinity but with reduced efficacy, resulting in weak partial agonists.[53]

A second development was aimed at increasing the potency of QMPSB (**1**) inspired by a series of compounds developed by Merck with a heterocyclic linker similar to (**12**) (tetrazole replaced by 1*H*-imidazole) but with the sulfamoyl tail replaced by a methylene unit. A significant increase in CB_1R potency was seen when replacing the piperidine moiety in (**15**) with 4,4-difluoropiperidine to give (**16**) (CB_1 EC_{50} = 320 and 25 nM, respectively). The monofluoro analog revealed a 3.5-fold drop in potency (CB_1 EC_{50} = 87 nM).[54] This observation inspired the use of 4,4-difluoropiperidine to generate 2F-QMPSB (QMDFPSB) (**17**) (Figure 1C). Testing carried out by SGT demonstrated potent psychoactive effects in human volunteers with a significant increase in potency compared to QMPSB (**1**) and also found that it was more stable to temperature with improved solubility. Despite the differences in core and head groups, a structural overlay can also be seen among the Merck compound (**16**), 2F-QMPSB (**17**), and AstraZeneca's AZD-1940 (**18**) (Figure 12).

Another novel compound utilized the isopropyl tail group as seen in compound (**11**), which was part of a series of compounds explored for their potential to afford increased CB_2R selectivity. As described earlier, compound (**8**) explored by Ermann and colleagues retained appreciable CB_1R activity. A change from the piperidine tail analog of (**11**) to the isopropyl tail group of (**11**) resulted in a reversal of selectivity (CB_1R EC_{50} = 228 nM; CB_2R EC_{50} = 2284),[48] inspiring the generation of QMiPSB (**19**) (Figure 1C) in an attempt to assess whether such increase in CB_1 selectivity and potency would occur. This compound was found to show reduced potency over QMPSB (**1**) though pharmacological confirmation on the desired CB_1R selectivity remains to be investigated.

A related derivative (**20**) closely related to Bay 38-7271 (**21**) developed by the Bayer AG, but with the same quinolin-8-yl head group motif seen in QMPSB (**1**) and PB-22 (**28**), demonstrated that

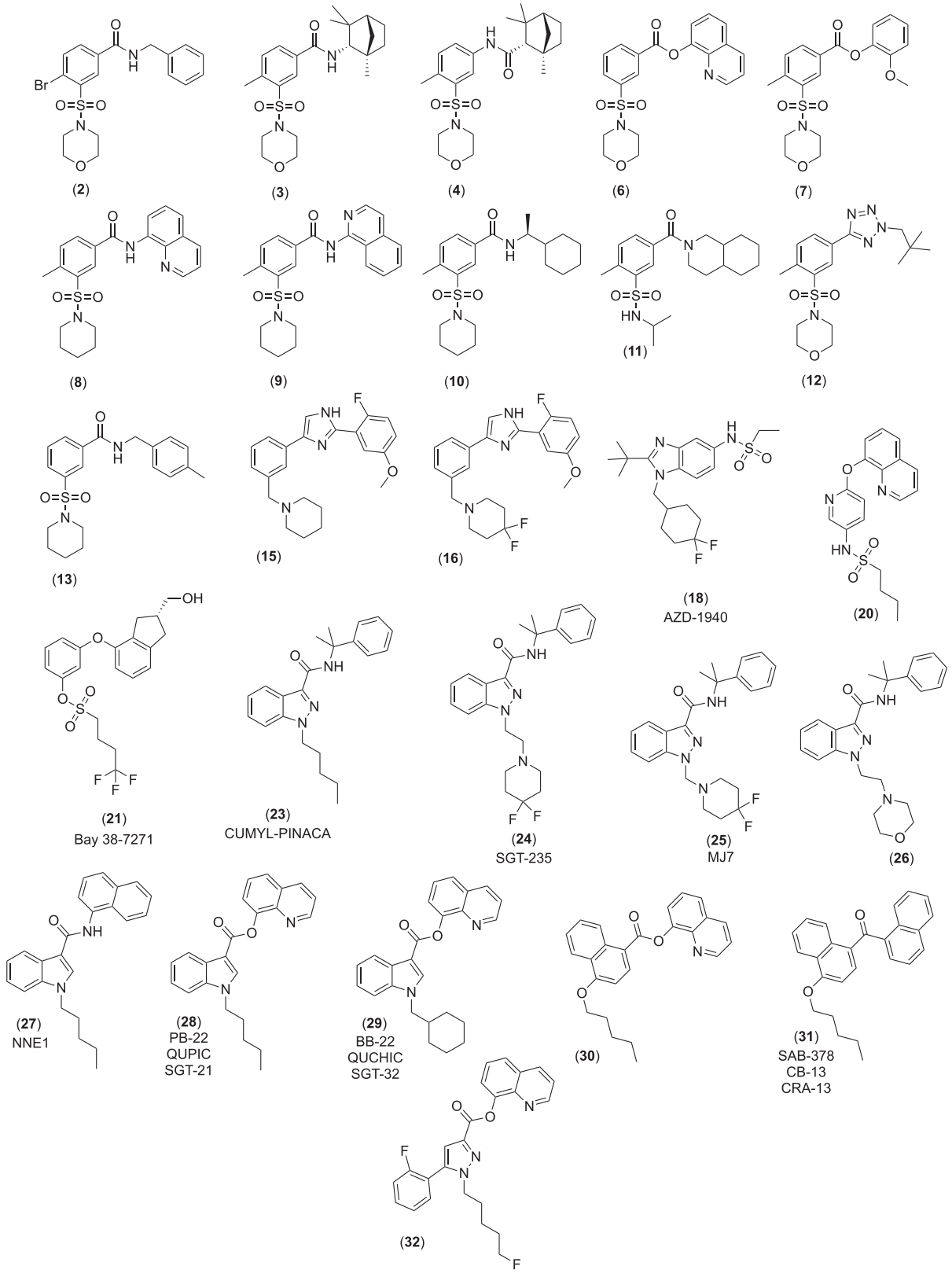

FIGURE 12 Chemical structures of cannabinoid receptor ligands including those informing the development of QMPCB (**14**), 2F-QMPSB (**17**), QMiPSB (**19**), SGT-233 (**22**) (Figure 1C) as potential new psychoactive substances

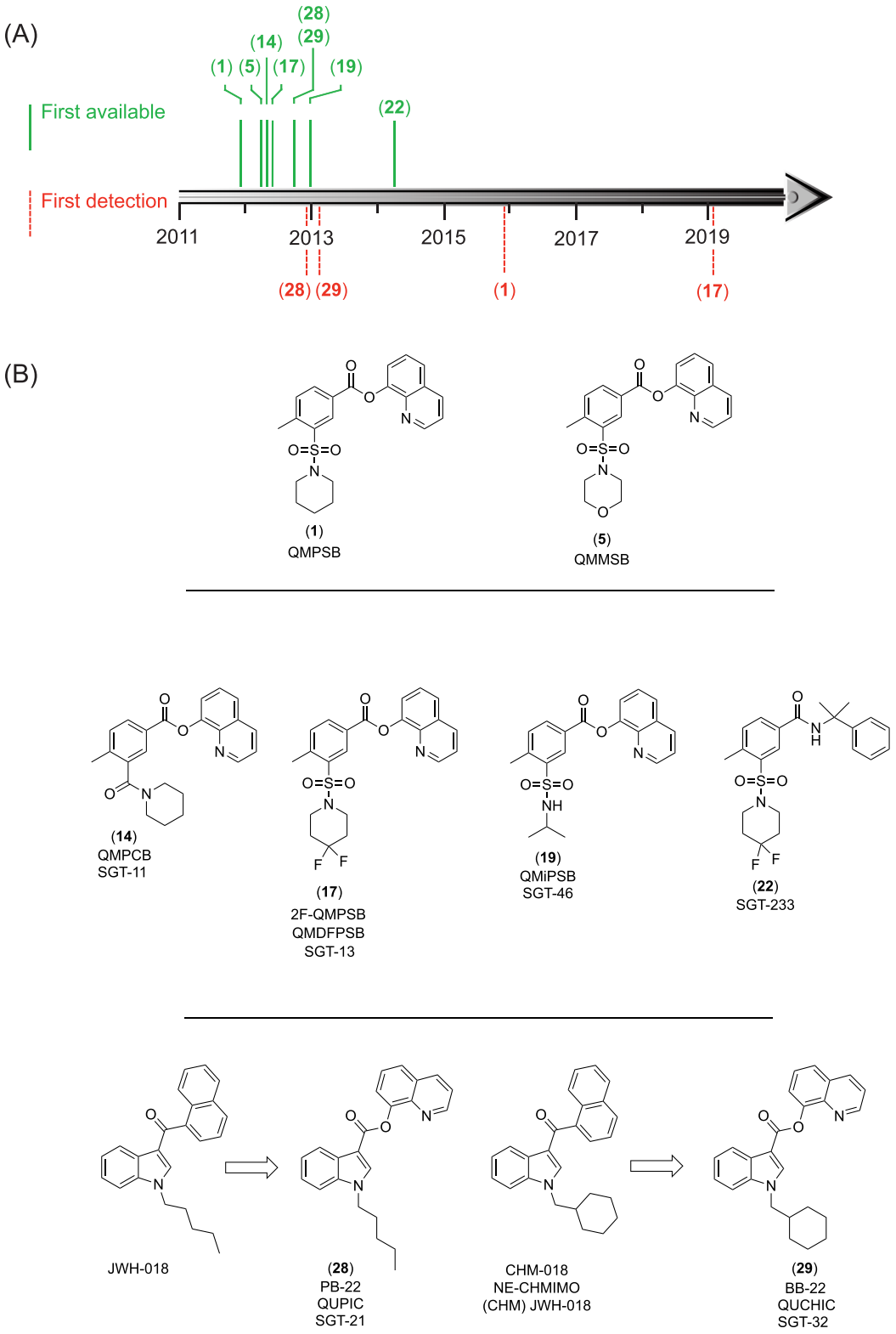

FIGURE 13 Historical perspective. A, Estimated timelines for availability and first reports of detection. Availability: QMPSB (**1**), November; QMMSB (**5**), March; QMPCB (**14**), April; 2F-QMPSB (**17**), May; QMiPSB (**19**), December; SGT-233 (**22**), March; PB-22 (**28**) and BB-22 (**29**), September 2012. First reported/published detections: (**1**) detected in methanol extracts of seized plant materials in 2011 and 2012 with the first appearance in a scientific publication in December 2015;[29] (**28**) and (**29**) detections first notified to the European Monitoring Centre for Drugs and Drug Addiction (EMCDDA) in November[49] and January[50] with the first appearance in a scientific publication in March 2013;[38] (**17**) detection first reported to EMCDDA in January 2019; herbal sample seized in January 2018.[51] B, QMPSB (**1**) and QMMSB (**5**) originated during pharmaceutical development and inspired a number of molecular hybridizations (**14**, **17**, **19**, and **22**), which also inspired the development of more prevalent synthetic cannabinoid receptor agonists such as PB-22 (**28**) and BB-22 (**29**) that emerged in 2012 [Colour figure can be viewed at wileyonlinelibrary.com]

this head group had been established as conferring useful CB_1 receptor binding as early as 1998.[55] Another derivative in this series was the cumylamide derivative SGT-233 (**22**) (Figure 1C). This was an attempt to combine the cumylamide head group seen in various potent indazole-3-carboxamide compounds such as CUMYL-PINACA (**23**)[56] with the 4,4-difluoropiperidine sulfamoyl motif of 2F-QMPSB (**17**) (Figure 1C). The replacement of the *n*-pentyl tail found in CUMYL-PINACA (**23**) with the 4,4-difluoropiperidine group, either being linked to the 1*H*-indazole nitrogen core via an ethylene or methylene unit, led to (**24**) (SGT-235 and MJ7 [**25**]).[56] The idea for the preparation of SGT-235 (**24**) arose from knowledge about the activity of CUMYL-MEINACA (**26**) (SGT-184), that is, 1-[2-(morpholin-4-yl) ethyl]-*N*-(2-phenylpropan-2-yl)-1*H*-indazole-3-carboxamide, and the availability of 4,4-difluoropiperidine from the 2F-QMPSB (**17**) synthesis. Compound (**25**), though mentioned in a patent application,[56] was apparently not synthesized at that time.

The similarity between SGT-233 (**22**) and the 1-cyclohexylethyl compound (**10**) also seems noteworthy. Compound (**22**) was found to be less potent than QMPSB (**1**) but similar in potency to the morpholine analog QMMSB (**5**) and more potent than (**14**) and (**19**). It is also worth noting that compound (**22**) showed an amide link rather than the ester as seen in the sulfamoyl benzoates (**1**), (**5**), (**14**), (**17**), and (**19**), which was a reflection of explorations published on a range of sulfamoyl benzamides with reduced potency compared to their benzoate counterparts.[47] Some structural similarity between cumyl analog (**22**) and (**13**) described earlier is also worth noting.

The second series of compounds derived from QMPSB (**1**) are those that utilized the quinolin-8-yl ester head group but combined this with the widely used *N*-alkyl 1*H*-indole or indazole core structure. These were primarily inspired by the indole-3-carboxamide derivative NNE1 (AM-6527, [carboxamide] JWH-018, MN-24) (**27**) (Figure 12), which was reported in 2011 by Blaazer et al. as a potent agonist at both CB_1 and CB_2 receptors (CB_1 K_i = 1.26 nM, EC_{50} = 10 nM, CB_2 K_i = 100 nM, EC_{50} = 7.94 nM).[57] Changing the naphthylamide head group of NNE1 to a quinolin-8-yl ester produced the potent CB_1 and CB_2 agonist PB-22 (QUPIC, SGT-21) (**28**) (EC_{50} = 5.1 nM at CB_1 and 37 nM at CB_2).[58] The related compound with a cyclohexylmethyl tail group BB-22 (**29**) (QUCHIC, SGT-32) is also a potent cannabinoid agonist (CB_1 K_i = 0.217 nM and CB_2 K_i = 0.338 nM)[59] and could be viewed to be more structurally similar to QMPSB (**1**). These compounds subsequently led to the development of a large series of related compounds with indole, 2-methylindole, indazole or 7-azaindole cores, ester or amide linkers, quinolin-8-yl or 1-naphthyl head groups, and a wide range of tail groups including pentyl, 5-fluoropentyl, 4-fluorobutyl, cyclohexylmethyl, (oxan-4-yl)methyl, benzyl, 4-fluorobenzyl, and 2-fluorophenyl groups. Only a limited amount of analytical and pharmacological data appear to be available for most of these compounds.

Though QMPSB (**1**) was identified from high-throughput screening efforts, it might be worth noting that the quinolin-8-yl ester group found in substances associated with cannabinoid research had been explored earlier. One example may be seen in (**30**) developed by Novartis AG (patent filed in 2001, example #38). A naphthyl methanone attachment was also explored in the pharmaceutical context.[15,60] This compound (**31**) (SAB-378, Figure 12) also became known as CB-13 and CRA-13 with detections being reported first in Japan[61] and Europe[62] in 2011.

As shown in the timeline in Figure 13A, the compounds investigated in the present study, that is, QMPSB (**1**), QMMSB (**5**), QMPCB (**14**), 2F-QMPSB (**17**), QMiPSB (**19**), and SGT-233 (**22**), became available as a research chemical between late 2011 and early 2014, whereas the detection of QMPSB (**1**) was published in 2016.[29] Though early investigations into sulfamoyl benzoates and benzamides carried out by Stargate International did not result in a significant appearance of compounds from these classes as NPS, the attachment of the quinolin-8-yl ester group on other core components led to the development of several widely reported compounds such as PB-22 (**28**) and BB-22 (**29**) (Figure 13A,B).

Future ideas for potentially unexplored SCRA candidates might however also come from more unusual sources. For example, the Texas State Legislature (USA) listed an ambiguously named compound defined as "quinolinyl fluoropentyl fluorophenyl pyrazole carboxylate,"[63] which could describe a range of isomeric compounds though one of the more plausible examples might be represented by (**32**) (Figure 12). Even though this compound (or corresponding isomers) does not yet appear to have been described in the scientific literature, it has been placed under control preemptively, possibly in the expectation that it might produce SCRA-like effects and thus be liable to abuse and illicit sale. Such "prophetic" compounds therefore represent another avenue by which new SCRAs might come into existence, especially, if such substances are revealed to be CB_1R/CB_2R agonists.

4 | CONCLUSIONS

In the present investigation, six SCRAs, that is, QMPSB (**1**), QMMSB (**5**), QMPCB (**14**), 2F-QMPSB (**17**), QMiPSB (**19**), and SGT-233 (**22**), were subjected to extensive analytical characterization. The majority of these data are reported for the first time. Implementation of GC- and LC-based techniques coupled with various ionization and (single and tandem) mass spectrometry platforms and spectroscopic analyses provided a complimentary set of key data including information on impurities. These data may be useful to researchers and scientists in cases where forensic and clinical investigations are warranted. Though the detection of QMPSB (**1**) was first published in 2016, Stargate International, a provider of research chemicals, investigated these six compounds and made them available between 2011 and early 2014. The impetus for exploring these particular compounds as research chemicals originated from QMPSB (**1**) and QMMSB (**5**) and many closely related compounds published in the scientific literature in 2007 that were under investigation as potential CB_2-selective receptor agonists. Structural modifications of QMPSB (**1**) investigated by Stargate International were informed by the information available from scientific data sources and applied to this "lead" compound. The rationale behind these assessments covered in this overview showed that QMPCB (**14**), 2F-QMPSB (**17**), QMiPSB (**19**), and SGT-233 (**22**)

were the results of these efforts. Though the information on the prevalence of use and availability related to QMPSB (**1**) and the remaining five compounds covered here is limited, one of the key outcomes of the research performed by Stargate International was to set the stage for the quinolin-8-yl ester head group that ultimately led to the hybridization with an *N*-alkyl-1*H*-indole core to yield SGT-21 and SGT-32, which became known as PB-22 and BB-22, respectively, thus opening the door to a range of SCRAs carrying the quinolin-8-yl head group from about 2012 onwards.

ACKNOWLEDGMENTS

The authors are grateful to Stephen J. Chapman (Isomer Design, Toronto, Canada) and Dr. István Ujváry for support and helpful comments on the manuscript.

ORCID

Simon D. Brandt https://orcid.org/0000-0001-8632-5372
Pierce V. Kavanagh https://orcid.org/0000-0002-1613-3305
Folker Westphal https://orcid.org/0000-0003-0452-7814
Geraldine Dowling https://orcid.org/0000-0001-8344-6582

REFERENCES

1. Bell MR. Sterling drug Inc., New York, USA. 3-Arylcarbonyl- and 3-cycloalkylcarbonyl-1-aminoalkyl-1*H*-indoles, compositions and use. US4581354A; 1986.
2. D'Ambra TE, Bell MR. Sterling Drubg Inc., New York, USA. 2- and 3-Aminomethyl-6-arylcarbonyl-2,3-dihydropyrrolo[1,2,3-de]-1,4-benzoxazines. US4939138A; 1990.
3. European Monitoring Centre for Drugs and Drug Addiction (EMCDDA). Synthetic cannabinoids in Europe (perspectives on drugs). EMCDDA, Lisbon, 2017. Available at: http://www.emcdda.europa.eu/system/files/publications/2753/POD_Syntheticcannabinoids_0.pdf [Accessed 31 March 2020].
4. Shevyrin V, Melkozerov V, Endres GW, Shafran Y, Morzherin Y. On a new cannabinoid classification system: a sight on the illegal market of novel psychoactive substances. *Cannabis Cannabinoid Res*. 2016;1(1):186-194.
5. Huffman JW, Padgett LW. Recent developments in the medicinal chemistry of cannabimimetic indoles, pyrroles and indenes. *Curr Med Chem*. 2005;12(12):1395-1411.
6. Manera C, Tuccinardi T, Martinelli A. Indoles and related compounds as cannabinoid ligands. *Mini Rev Med Chem*. 2008;8(4):370-387.
7. Wiley JL, Marusich JA, Huffman JW. Moving around the molecule: relationship between chemical structure and in vivo activity of synthetic cannabinoids. *Life Sci*. 2014;97(1):55-63.
8. Banister SD, Connor M. The chemistry and pharmacology of synthetic cannabinoid receptor agonists as new psychoactive substances: origins. *Handb Exp Pharmacol*. 2018;252:165-190.
9. Banister SD, Connor M. The chemistry and pharmacology of synthetic cannabinoid receptor agonists as new psychoactive substances: evolution. *Handb Exp Pharmacol*. 2018;252:191-226.
10. Alam RM, Keating JJ. Adding more "spice" to the pot: a review of the chemistry and pharmacology of newly emerging heterocyclic synthetic cannabinoid receptor agonists. *Drug Test Anal*. 2020;12(3):297-315.
11. Buchler IP, Hayes MJ, Hegde SG, et al. Pfizer Inc., New York, USA. Indazole derivatives. WO2009106980A2; 2009.
12. Buchler IP, Hayes MJ, Hegde SG, et al. Pfizer Inc., New York, USA. Indazole derivatives. WO2009106982A1; 2009.
13. Banister SD, Longworth M, Kevin R, et al. Pharmacology of valinate and *tert*-leucinate synthetic cannabinoids 5F-AMBICA, 5F-AMB, 5F-ADB, AMB-FUBINACA, MDMB-FUBINACA, MDMB-CHMICA, and their analogues. *ACS Chem Nerosci*. 2016;7(9):1241-1254.
14. Shevyrin V, Melkozerov V, Nevero A, et al. Identification and analytical characteristics of synthetic cannabinoids with an indazole-3-carboxamide structure bearing a *N*-1-methoxycarbonylalkyl group. *Anal Bioanal Chem*. 2015;407(21):6301-6315.
15. Brain CT, Culshaw AJ, Dziadulewicz EK, Schopfer U. Novartis AG, Basel, Switzerland. Naphthalene derivatives. WO0242248A2; 2002.
16. Pace JM, Tietje K, Dart MJ, Meyer MD. Abbott Laboratories, Illinois, USA. 3-Cycloalkylcarbonyl indoles as cannabinoid receptor ligands. WO2006069196A1; 2006.
17. Florjancic AS, Dart MJ, Ryther KB, et al. Abbott Laboratories, Illinois, USA. Novel compounds as cannabinoid receptor ligands and uses thereof. US20080058335A1; 2008.
18. Uchiyama N, Kawamura M, Kikura-Hanajiri R, Goda Y. URB-754: a new class of designer drug and 12 synthetic cannabinoids detected in illegal products. *Forensic Sci Int*. 2013;227(1–3):21-32.
19. Uemura N, Fukaya H, Kanai C, et al. Identification of a synthetic cannabinoid A-836339 as a novel compound found in a product. *Forensic Toxicol*. 2014;32(1):45-50.
20. Uchiyama N, Asakawa K, Kikura-Hanajiri R, Tsutsumi T, Hakamatsuka T. A new pyrazole-carboxamide type synthetic cannabinoid AB-CHFUPYCA [*N*-(1-amino-3-methyl-1-oxobutan-2-yl)-1-(cyclohexylmethyl)-3-(4-fluorophenyl)-1*H*-pyrazole-5-carboxamide] identified in illegal products. *Forensic Toxicol*. 2015;33(2):367-373.
21. McLaughlin G, Morris N, Kavanagh PV, et al. The synthesis and characterization of the 'research chemical' *N*-(1-amino-3-methyl-1-oxobutan-2-yl)-1-(cyclohexylmethyl)-3-(4-fluorophenyl)-1*H*-pyrazole-5-carboxamide (3,5-AB-CHMFUPPYCA) and differentiation from its 5,3-regioisomer. *Drug Test Anal*. 2016;8(9):920-929.
22. Girreser U, Rösner P, Vasilev A. Structure elucidation of the designer drug *N*-(1-amino-3,3-dimethyl-1-oxobutan-2-yl)-1-(5-fluoropentyl)-3-(4-fluorophenyl)-pyrazole-5-carboxamide and the relevance of predicted 13C NMR shifts – a case study. *Drug Test Anal*. 2016;8(7):668-675.
23. Jia W, Meng X, Qian Z, Hua Z, Li T, Liu C. Identification of three cannabimimetic indazole and pyrazole derivatives, APINACA 2*H*-indazole analogue, AMPPPCA, and 5F-AMPPPCA. *Drug Test Anal*. 2017;9(2):248-255.
24. Pertwee RG. Inverse agonism and neutral antagonism at cannabinoid CB_1 receptors. *Life Sci*. 2005;76(12):1307-1324.
25. Wiley JL, Jefferson RG, Grier MC, Mahadevan A, Razdan RK, Martin BR. Novel pyrazole cannabinoids: insights into CB_1 receptor recognition and activation. *J Pharmacol Exp Ther*. 2001;296(3):1013-1022.
26. Yildirim M, Wals HC, van Vliet BJ, Lange JHM. Solvay pharmaceuticals B.V., Weesp, the Netherlands. 4,5-Dihydro-(1*H*)-pyrazole derivatives as cannabinoid CB1 receptor modulators. WO2008152086A2; 2008.
27. Lange JHM, Zilaout H, van Vliet BJ. Solvay pharmaceuticals B.V., Weesp, the Netherlands. 5-Aryl-4,5-dihydro-(1*H*)-pyrazoles as cannabinoid CB1 receptor agonists. WO2009037244A2; 2009.
28. Balasubramanian G, Gullapalli S, Joshi NK, Muthuppalaniappan M, Narayanan S. Glenmark Pharmaceuticals S.A., La Chaux-De-Fonds, Switzerland. Novel cannabinoid receptor ligands, pharmaceutical compositions containing them, and process for their preparation. WO2006129178A1; 2006.
29. Blakey K, Boyd S, Atkinson S, et al. Identification of the novel synthetic cannabimimetic 8-quinolinyl 4-methyl-3-(1-piperidinylsulfonyl) benzoate (QMPSB) and other designer drugs in herbal incense. *Forensic Sci Int*. 2016;260:40-53.

30. Dawson PH, Sun W-F. A round robin on the reproducibility of standard operating conditions for the acquisition of library MS/MS spectra using triple quadrupoles. *Int J Mass Spectrom Ion Processes*. 1984; 55(2):155-170.
31. Response. Analytical report. 2F-QMPSB (C22H20F2N2O4S). Sample ID: 2109–19. National Forensic Laboratory, Ljubljana, Slovenia. 2019. Available at: https://www.policija.si/apps/nfl_response_web/0_Analytical_Reports_final/2F-QMPSB-ID-2109-19_report.pdf [13 April 2020].
32. Blumenthal T, Gillis RG, Porter QN, Yeoh LL. Elimination of carbon monoxide by electron impact on quinoline *N*-oxide, carbostyril and 8-hydroxyquinoline. *Org Mass Spectrom*. 1991;26(4):247-249.
33. Richter WJ, Schwarz H. Chemical ionization - a mass-spectrometric analytical procedure of rapidly increasing importance. *Angew Chem Int Ed*. 1978;17(6):424-439.
34. Zhang W, Luo M. Iron-catalyzed synthesis of arylsulfinates through radical coupling reaction. *Chem Commun*. 2016;52(14):2980-2983.
35. Zhu H, Shen Y, Deng Q, Tu T. Copper-catalyzed electrophilic amination of sodium sulfinates at room temperature. *Chem Commun*. 2015;51(92):16573-16576.
36. Hirsch JA, Augustine RL, Koletar G, Wolf HG. Barriers to amide rotation in piperidides and related systems. Unambiguous assignments using carbon-13 magnetic resonance. *J Org Chem*. 1975;40(24):3547-3550.
37. Li W, Wu X-F. Palladium-catalyzed aminocarbonylation of *N*-chloroamines with boronic acids. *Chem A Eur J*. 2015;21(20):7374-7378.
38. Uchiyama N, Matsuda S, Kawamura M, Kikura-Hanajiri R, Goda Y. Two new-type cannabimimetic quinolinyl carboxylates, QUPIC and QUCHIC, two new cannabimimetic carboxamide derivatives, ADB-FUBINACA and ADBICA, and five synthetic cannabinoids detected with a thiophene derivative α-PVT and an opioid receptor agonist AH-7921 identified in illegal products. *Forensic Toxicol*. 2013;31(2): 223-240.
39. Liu C, Jia W, Hua Z, Qian Z. Identification and analytical characterization of six synthetic cannabinoids NNL-3, 5F-NPB-22-7N, 5F-AKB-48-7N, 5F-EDMB-PINACA, EMB-FUBINACA, and EG-018. *Drug Test Anal*. 2017;9(8):1251-1261.
40. Tanaka Y, Tanaka Y. Infrared absorption spectra of organic sulfur compounds. I. Studies on S-*N* stretching bands of benzenesulfonamide derivatives. *Chem Pharm Bull*. 1965;13(4):399-405.
41. Tsujikawa K, Yamamuro T, Kuwayama K, Kanamori T, Iwata YT, Inoue H. Thermal degradation of a new synthetic cannabinoid QUPIC during analysis by gas chromatography-mass spectrometry. *Forensic Toxicol*. 2014;32(2):201-207.
42. Thomas BF, Lefever TW, Cortes RA, et al. Thermolytic degradation of synthetic cannabinoids: chemical exposures and pharmacological consequences. *J Pharmacol Exp Ther*. 2017;361(1):162-171.
43. Dolle RE, Worm K, Zhou QJ. Adolor corporation, Exton, Pennsylvania, USA. Sulfamoyl benzamide derivatives and methods of their use. US7297796B2; 2007.
44. Dolle RE, Worm K. Adolor corporation, Exton, Pennsylvania, USA. Sulfamoyl benzamides as cannabinoid receptor modulators. WO2007/058960; 2007.
45. Worm K, Zhou QJ, Saeui CT, et al. Sulfamoyl benzamides as novel CB_2 cannabinoid receptor ligands. *Bioorg Med Chem Lett*. 2008;18(9): 2830-2835.
46. Goodman AJ, Ajello CW, Worm K, et al. CB2 selective sulfamoyl benzamides: optimization of the amide functionality. *Bioorg Med Chem Lett*. 2009;19(2):309-313.
47. Lambeng N, Lebon F, Christophe B, Burton M, De Ryck M, Quéré L. Arylsulfonamides as a new class of cannabinoid CB1 receptor ligands: identification of a lead and initial SAR studies. *Bioorg Med Chem Lett*. 2007;17(1):272-277.
48. Ermann M, Riether D, Walker ER, et al. Arylsulfonamide CB2 receptor agonists: SAR and optimization of CB2 selectivity. *Bioorg Med Chem Lett*. 2008;18(5):1725-1729.
49. European Monitoring Centre for Drugs and Drug Addiction (EMCDDA). EMCDDA–Europol 2012 annual report on the implementation of council decision 2005/387/JHA (new drugs in Europe, 2012). EMCDDA, Lisbon, 2013. Available at: https://www.emcdda.europa.eu/system/files/publications/734/EMCDDA-Europol_2012_Annual_Report_final_439477.pdf [Accessed 31 March 2020].
50. European Monitoring Centre for Drugs and Drug Addiction (EMCDDA). EMCDDA–Europol 2013 annual report on the implementation of council decision 2005/387/JHA. EMCDDA, Lisbon, 2014. Available at: https://www.emcdda.europa.eu/system/files/publications/814/TDAN14001ENN_475519.pdf [Accessed 31 March 2020].
51. European Monitoring Centre for Drugs and Drug Addiction (EMCDDA). Early warning system formal notification. Date issued: 10 January 2019. RCS ID: EU-EWS-RCS-FN-2019-0002.Formal notification of quinolin-8-yl 3-((4,4-difluoropiperidin-1-yl)sulfonyl)-4-methylbenzoate (2F-QMPSB) by Italy as a new psychoactive substance under the terms of Regulation (EU) 2017/2101. 2019.
52. Sitkoff DF, Lee N, Ellsworth BA, et al. Cannabinoid CB_1 receptor ligand binding and function examined through mutagenesis studies of F200 and S383. *Eur J Pharmacol*. 2011;651(1–3):9-17.
53. Banister SD, Krishna Kumar K, Kumar V, Kobilka BK, Malhotra SV. Selective modulation of the cannabinoid type 1 (CB_1) receptor as an emerging platform for the treatment of neuropathic pain. *MedChemComm*. 2019;10(5):647-659.
54. Yang S-W, Smotryski J, Matasi J, et al. Structure–activity relationships of 2,4-diphenyl-1*H*-imidazole analogs as CB2 receptor agonists for the treatment of chronic pain. *Bioorg Med Chem Lett*. 2011;21(1): 182-185.
55. Mittendorf J, Dressel J, Matzke M, et al. Bayer AG, Leverkusen, Germany. Arylsulfonamide und Analoga und ihre Verwendung zur Behandlung von neurodegenerativen Erkrankungen. WO199837061; 1998.
56. Bowden MJ, Williamson JPB. Auckland, New Zealand. Cannabinoid compounds. WO2014167530A1; 2014.
57. Blaazer AR, Lange JH, van der Neut MA, et al. Novel indole and azaindole (pyrrolopyridine) cannabinoid (CB) receptor agonists: design, synthesis, structure-activity relationships, physicochemical properties and biological activity. *Eur J Med Chem*. 2011;46(10):5086-5098.
58. Banister SD, Stuart J, Kevin RC, et al. Effects of bioisosteric fluorine in synthetic cannabinoid designer drugs JWH-018, AM-2201, UR-144, XLR-11, PB-22, 5F-PB-22, APICA, and STS-135. *ACS Chem Nerosci*. 2015;6(8):1445-1458.
59. Hess C, Schoeder CT, Pillaiyar T, Madea B, Muller CE. Pharmacological evaluation of synthetic cannabinoids identified as constituents of spice. *Forensic Toxicol*. 2016;34(2):329-343.
60. Dziadulewicz EK, Bevan SJ, Brain CT, et al. Naphthalen-1-yl-(4-pentyloxynaphthalen-1-yl)methanone: a potent, orally bioavailable human CB_1/CB_2 dual agonist with antihyperalgesic properties and restricted central nervous system penetration. *J Med Chem*. 2007;50 (16):3851-3856.
61. Yoshida M, Suzuki J, Nakajima J, et al. Analysis of illegal drugs purchased in the fiscal year 2011. *Ann Rep Tokyo Metr Inst Pub Health*. 2012;63:111-124.
62. European Monitoring Centre for Drugs and Drug Addiction (EMCDDA). EMCDDA–Europol 2011 annual report on the implementation of council decision 2005/387/JHA. In accordance with Article 10 of Council Decision 2005/387/JHA on the information exchange, risk assessment and control of new psychoactive substances. EMCDDA, Lisbon, 2012. Available at: http://www.emcdda.europa.

eu/system/files/publications/689/EMCDDA-Europol_Annual_Report_2011_2012_final_335568.pdf [Accessed 31 March 2020].
63. Anonymous. Texas health and safety code § 481.1031. Penalty group 2-a. http://codes.findlaw.com/tx/health-and-safety-code/health-safety-sect-481-1031.html. [Accessed 01 July 2018]

SUPPORTING INFORMATION

Additional supporting information may be found online in the Supporting Information section at the end of this article.

How to cite this article: Brandt SD, Kavanagh PV, Westphal F, et al. Synthetic cannabinoid receptor agonists: Analytical profiles and development of QMPSB, QMMSB, QMPCB, 2F-QMPSB, QMiPSB, and SGT-233. *Drug Test Anal*. 2021;13: 175–196. https://doi.org/10.1002/dta.2913